

This is an Open Access document downloaded from ORCA, Cardiff University's institutional repository: <https://orca.cardiff.ac.uk/id/eprint/159170/>

This is the author's version of a work that was submitted to / accepted for publication.

Citation for final published version:

Mangano, Giacomo, Alves, Tiago M. , Zecchin, Massimo, Civile, Dario and Critelli, Salvatore 2023. The Rossano-San Nicola Fault Zone evolution impacts the burial and maturation histories of the Crotone Basin, Calabrian Arc, Italy. *Petroleum Geoscience* 29 (2) , petgeo2022-085. 10.1144/petgeo2022-085

Publishers page: <http://dx.doi.org/10.1144/petgeo2022-085>

Please note:

Changes made as a result of publishing processes such as copy-editing, formatting and page numbers may not be reflected in this version. For the definitive version of this publication, please refer to the published source. You are advised to consult the publisher's version if you wish to cite this paper.

This version is being made available in accordance with publisher policies. See <http://orca.cf.ac.uk/policies.html> for usage policies. Copyright and moral rights for publications made available in ORCA are retained by the copyright holders.



Accepted Manuscript

Petroleum Geoscience

The Rossano-San Nicola Fault Zone evolution impacts the burial and maturation histories of the Crotona Basin, Calabrian Arc, Italy

Giacomo Mangano, Tiago M. Alves, Massimo Zecchin, Dario Civile & Salvatore Critelli

DOI: <https://doi.org/10.1144/petgeo2022-085>

To access the most recent version of this article, please click the DOI URL in the line above. When citing this article please include the above DOI.

Received 31 October 2022

Revised 13 April 2023

Accepted 17 April 2023

© 2023 The Author(s). Published by The Geological Society of London for GSL and EAGE. All rights reserved. For permissions: <http://www.geolsoc.org.uk/permissions>. Publishing disclaimer: www.geolsoc.org.uk/pub_ethics

Manuscript version: Accepted Manuscript

This is a PDF of an unedited manuscript that has been accepted for publication. The manuscript will undergo copyediting, typesetting and correction before it is published in its final form. Please note that during the production process errors may be discovered which could affect the content, and all legal disclaimers that apply to the journal pertain.

Although reasonable efforts have been made to obtain all necessary permissions from third parties to include their copyrighted content within this article, their full citation and copyright line may not be present in this Accepted Manuscript version. Before using any content from this article, please refer to the Version of Record once published for full citation and copyright details, as permissions may be required.

The Rossano-San Nicola Fault Zone evolution impacts the burial and maturation histories of the Croton Basin, Calabrian Arc, Italy

Giacomo Mangano^{a, b}, Tiago M. Alves^c, Massimo Zecchin^b, Dario Civile^b, Salvatore Critelli^a

a Department of Environmental Engineering, University of Calabria, 87036, Arcavacata di Rende, CS, Italy

b National Institute of Oceanography and Applied Geophysics – OGS, 34010 Sgonico, TS, Italy

c 3D Seismic Laboratory – School of Earth and Environmental Sciences, Cardiff University, CF10 3AT, United Kingdom

Highlights

- Contractual and extensional tectonics in the Croton Basin relate to the development of the Ionian and Tyrrhenian Seas
- Early Langhian contractional/transpressional tectonics generated new structural traps
- Pliocene (Zanclean-Piacenzian) tectonics led to the emplacement of large mass-transport complexes
- Pliocene tectonics impacted source-rock maturation in the Croton Basin

Abstract

This work addresses the tectonic significance of a NW-SE strike-slip fault zone in the Calabrian Arc of Southern Italy, the Rossano-San Nicola Fault Zone (RSFZ). High-quality seismic reflection and 1D forward models of exploration boreholes and pseudo-wells show that the RSFZ experienced multiple Miocene phases of contractional/transpressional tectonics. These were followed by crustal extension during the Pliocene in association with the oceanisation of the Tyrrhenian Sea, Apennine orogenesis, and collision between the Calabrian Arc and adjacent tectonic plates. Such a setting had a profound influence on the Croton Basin and its economic potential: 1) tectonic reactivation allowed reservoir units of the Croton Basin to be charged by gas derived from Triassic/Lower Jurassic source rocks, and 2) source rocks reached their maximum depth and remained in the gas generation window after the emplacement of a large mass-transport complex in the Pliocene. In the surrounding areas, tectonic activity near the RSFZ contributed to source-rock maturation by enhancing local sedimentation rates, particularly during Langhian (Middle Miocene) and Zanclean (early Pliocene) tectonics. This work is important as it demonstrates the tectono-stratigraphic evolution of the Croton Basin to be closely related to the structural evolution of the RSFZ. Crucially, the study area reveals the first example of a gas field fully sealed by a large mass-transport complex. As a corollary, we tie the Late Cenozoic geological history of the Croton Basin to the geodynamic evolution of the central Mediterranean region, namely the Ionian and Tyrrhenian seas. We identify new prospects in the Croton Basin and provide a time frame for gas generation and accumulation in Southern Italy.

Keywords: Adria Plate; Calabrian Terranes; Croton Basin; Strike-slip tectonics; Burial history

1. Introduction

Tectono-stratigraphic analyses of sedimentary basins are paramount to understand their economic potential, namely the importance of discrete tectonic episodes on the 4D evolution of petroleum systems (Alves *et al.*, 2020). Such analyses require a holistic approach and the use of vast datasets to address the formation, infill and erosion of sedimentary basins, information deemed crucial to later discern their tectonic settings, palaeogeography and subsidence histories (Fraser, 2010). In detail, tectonic movements may have a mixed economic impact by positively affecting the formation of structural traps, while negatively controlling the timing of fluid migration (Tari *et al.*, 2020). At the same time, local and far-field tectonics can enhance seal competence, while leading to the exhumation (or excessive burial) of source rocks in different parts of sedimentary basins (Maerten *et al.*, 2019; Tari *et al.*, 2020). The fast and widespread accumulation of strata - including mass-transport complexes - during discrete tectonic episodes is known to enhance source-rock maturation, promoting the trapping of hydrocarbons in the slope depocentres where such mass-wasted strata are known to rest (Zhao *et al.*, 2015; Sun *et al.*, 2017). Conversely, the source areas of mass-transport complexes often record important migration (loss) of fluid to the surface via the sudden release of confining overburden pressure (Alves, 2010; Alves, 2015).

Part of a Late Cenozoic forearc depocentre of the Ionian arc-trench system, the Croton Basin has been recognised as an important natural gas province since the 1970s (Roveri *et al.*, 1992). (Fig. 1). Known gas fields span the onshore to near-offshore areas of the Croton Basin near the culmination of compressional, or contractional, structures (Fig. 1). The geological evolution of this basin has also been controlled by NW-SE strike-slip faults since the Late Cenozoic, and some of these structures were reactivated concomitantly with the accumulation of large mass-transport deposits in its offshore part (Massari and Prosser, 2013; Zecchin *et al.*, 2015; 2018; 2020; Critelli, 2018; Mangano *et al.*, 2020; 2021). Reliable

stratigraphic information already exists for reservoir units in the Croton Basin (Roveri *et al.*, 1992), but data on the evolution of these NW-SE strike-slip faults is lacking in the published literature. Similarly, as the maturation history of potential source rocks and the timing(s) of hydrocarbon generation are still to be fully addressed, the aims of this study are to investigate:

- a) the tectono-stratigraphic evolution of the Calabrian offshore area (Southern Italy) from the Triassic to the present day;
- b) the burial and thermal histories of the Croton Basin, with emphasis given to known source rock intervals;
- c) the formation of particular seal intervals and structural traps relative to the development of NW-SE strike-slip fault zones in the Croton Basin.

At the end of this work, we will tie the evolution of the latter fault zones to key geodynamic events recorded in the Central Mediterranean region. Finally, we will compare the results of this study with Roveri *et al.* (1992), who considered reservoir units in the study area to occur below a regional compressive structure related to a Pliocene tectonic phase.

2. Geological setting

2.1 Tectonic evolution of the Western and Central Mediterranean regions

The Ionian Sea is an oceanic basin located between the Apulian and the Malta escarpments, connecting the Eastern Mediterranean with the oceanic domain of North Africa (Fig. 1). It was first developed during Neotethys' continental rifting, which resulted in the

fragmentation of the Mediterranean region in multiple tectonic (micro)plates, e.g. Mesomediterranean (e.g., Critelli *et al.*, 2008; Critelli, 2018; Critelli and Martin-Martin, 2022), Iberia, AlKaPeCa, Adria, Eurasia, Africa, and Hellenic-Turkey plates (Stampfli and Marchant, 1997; Catalano *et al.*, 2000; Handy *et al.*, 2010; Van Hinsenberg *et al.*, 2020). These tectonic plates bordered the Alpine Tethys, Liguro-Piedmont, Valais and Lagonegro oceans (Stampfli, 2005). Near the study area, the Lagonegro Ocean has been previously recognised as forming the western extension of the Ionian Sea (Critelli *et al.*, 1999).

Continental rifting started at the end of the Permian in what is now the Ionian Sea and evolved towards oceanic spreading in the Late Jurassic-Early Cretaceous (Catalano *et al.*, 2001). The opening of the Ionian Sea is itself inferred to have resulted from Early-Middle Jurassic lateral motion between Adria and Africa, which formed a seaway between the North Atlantic seaway to the NW and the Neotethys to the SE (Channell *et al.*, 2022). In the Late Jurassic, Adria and Africa became joined, interrupting tectonic extension in the Ionian region (Fig. 2). On a more regional scale, the Ionian Sea as an oceanic realm was developed during the Late Jurassic-Early Cretaceous left-lateral motion of Iberia with respect to Eurasia, due to the eastward drift and counterclockwise rotation of the former during the opening of the Bay of Biscay (Vissers and Meijer, 2012; Angrand *et al.* 2020). At the time, the resulting deformation was accommodated across a ~ 400 km wide region extending from the Iberian Chain System in the SW, to the Armorican Shelf/Northern Aquitaine systems in the NE, along the so-called Iberia/Eurasia plate boundary (Angrand *et al.* 2020).

The oceanisation process ceased in the Ionian Sea during the Late Cretaceous due to a change from divergent to convergent tectonics in the context of collision between Africa and Eurasia – the so-called Alpine orogenesis (Critelli, 1993; Stampfli and Marchant, 1997; Critelli, 1999; Stampfli and Finetti, 2005; Stampfli and Hochard, 2009). During Africa-Eurasia convergence, Iberia became separated from Corsica and the Stilo-Aspromonte-

Peloritan Block by a right-lateral transform fault (Stampfli and Hochard, 2009). Later, Paleogene plate convergence continued to affect the Mediterranean region, and southern Italy, resulting in the subduction of Apulia-Adria beneath Iberia (Mesoalpine phase).

In the Middle Miocene (Langhian), the Tyrrhenian Sea was closed juxtaposing the Calabria-Peloritani Block (Stilo-Aspromonte-Peloritan and Africo-Polsi units) against the Corsica-Sardinia Block. The Ionian Sea pinched out westward, to the east of the Inner Carbonate platform and Apenninic Platform (Van Hinsbergen *et al.*, 2020) (Fig. 2). At present, the Ionian Sea is bounded to the W by the Calabrian Arc, which has been rifted away from Sardinia since the Middle Miocene (Serravallian in Mattei *et al.*, 2002).

After the Serravallian, the Calabrian Arc is known to have migrated rapidly (up to 6-8 cm/yr) to its present position between Sicily and the southern Apennine Range, in response to the ongoing oceanisation of the Tyrrhenian Sea (Massari and Prosser, 2013). Rapid slab rollback of the Ionian plate is currently regarded as having been, since the Serravallian, the main driving force of Tyrrhenian Sea opening. As a result, backarc opening has occurred in the Tyrrhenian region in the form of intermittent episodes of crustal stretching, which generated localised spreading centres at 4–5 Ma (Vavilov Basin) and 2.1–1.6 Ma (Marsili Basin). Moreover, the direction of crustal stretching changed through time; it was E-W during the Tortonian to early Pliocene and became oriented NW–SE in the Late Pliocene to early Pleistocene (Sartori, 2003).

At present, the evolution of the study area (Crotone Basin) is still closely related to the southeast migration of the Calabrian terranes under a setting dominated by Ionian plate subduction, associated slab roll-back, and Tyrrhenian Sea extension (Fig. 1). These events have led to the formation of NW- and WNW-ESE strike-slip fault zones, which fragmented the Calabrian Arc in multiple blocks (Tansi *et al.*, 2007; Verges *et al.*, 2012; Jolivet *et al.*, 2021a). Within such a background, the Rossano-San Nicola Fault Zone (RSFZ) is, in the

study area, one of such major NW- and WNW-ESE strike-slip fault zones and crosses the northern boundary of the Crotona Basin (Figs. 1 and 2).

2.2 Stratigraphic successions of the Central Mediterranean Sea

Due to its key location in the broader Mediterranean Sea, Mesozoic-Cenozoic strata in the Ionian Sea documents multi-phased continental rifting (Triassic to Early Jurassic), Tethyan continental breakup, and a period of open-ocean conditions (Early Jurassic to Early Cretaceous). Tethyan subduction and the onset of Alpine orogenesis occurred from Late Cretaceous to the Paleogene, Adria (or Apennines) orogenesis from the Early Miocene to the present day, and, finally, Tyrrhenian Sea's back-arc rifting (the so-called Tyrrhenian phase) from 15 Ma to the present day. Importantly, Mesozoic strata deposited in the older Tethys Ocean contain black shales deposited during the Triassic, Jurassic and Cretaceous Oceanic Anoxic Events (OAEs); they are the principal source rocks in known petroleum systems of the modern Mediterranean Sea (Jenkins, 1980; Jenkins, 1999).

Still in the Ionian region, terrestrial red beds of Triassic age lie unconformably over granodiorites, gneisses and phyllites, which comprise the basement rocks of the Calabrian Arc (Zuffa *et al.*, 1980; Santantonio and Teale, 1987; Critelli *et al.*, 2008; Critelli *et al.*, 2016 – Foglio 590 Taurianova) (Fig. 3). These red beds are overlain by Jurassic shallow-water, slope and basin carbonates, and other siliciclastic sediments (Zuffa *et al.*, 1980; Santantonio and Teale, 1987) (Fig. 3). Above these red beds are prominent Jurassic and Cretaceous inner- (Alburni-Cervati-Pollino-Panormide) and outer- (Apulia) platform carbonates, ranging from 1000 m to 2000 m in thickness. Also documented in this Cretaceous sequence are clays, marls and shales, pelagic carbonates and cherty limestones, reworked coarse-grained

carbonates/clastic turbidites and gravity flows. A siliciclastic Calabrian Flysch Unit ends the Mesozoic to Early Cenozoic stratigraphic succession of the Ionian Sea – it reflects the regional geodynamic changes that resulted from Paleogene subduction of Apulia-Adria beneath Iberia (Fig. 3). Therefore, the resulting Calabrian Arc comprises, offshore, a nappe stack of metamorphic and sedimentary units that are part of the so-called Calabrian Accretionary Wedge, or Complex (Rossetti et al., 2004; Sartori *et al.*, 2004) (Fig. 1).

Serravallian to Pleistocene strata of the Crotona Basin - a forearc depocenter located in a wedge-top position near the Calabrian Arc - lies unconformably above the Mesozoic-Lower Cenozoic sedimentary successions of the study area. The sedimentary succession of the Crotona Basin starts with coarse-grained breccias deposited by alluvial fans, which change seawards into fan-delta conglomerates (San Nicola Formation; Serravallian; Fig. 4). The San Nicola Formation is itself overlain by the silts and intercalated sands of the Ponda Group (Tortonian), which represents shelf to slope facies (Zecchin et al., 2020) (Fig. 4). While the base of the Crotona Basin's sediments is marked by a Serravallian Unconformity (SU), the Serravallian and Tortonian are separated by a Tortonian Unconformity (TU) (Fig. 4). Both unconformities are associated with important tectonic tilting of the Crotona Basin's shoulder (Zecchin et al., 2020).

Serravallian-Tortonian strata in the Crotona Basin are sealed by a Messinian succession composed of diatomites (Tripoli Formation), halite and resedimented evaporites (Evaporite Formation), limestones, siliciclastic sandstones (Petilia-Policastro Formation), conglomerates and mudstones (Carvane Group), reflecting continental to continental-slope depositional environments (Zecchin et al., 2020) (Fig. 4). An intra-Messinian Unconformity (IMU) separates the Evaporite and the Petilia Policastro formations, while an Upper Messinian Unconformity (UMU) bounds the Petilia-Policastro Formation from the Carvane Group (Fig. 4). In the literature, the IMU has been associated to isostatic rebound due to the Messinian

Salinity Crisis, while the UMU results from tectonic collision between the Calabrian Arc and the Apulian margin, located to the NE of this latter arc (Zecchin et al., 2020).

Plio-Pleistocene deposits complete the Crotona Basin's stratigraphy (Fig. 4). Seawards, they comprise the silty Cavalieri Marl (Zanclean), reflecting deep-water conditions, and the Cutro Clay (Piacenzian to Pleistocene) (Fig. 4). Towards the basin shoulder, the Cavalieri Marl and the Cutro Clay interfinger with sandy and gravelly intervals in the Zinga Sandstone and Belvedere Formation (Zanclean), the Scandale Sandstones (Piacenzian/early Gelasian), and the San Mauro Sandstones and Serra Mulara Formation (Middle Pleistocene) (Fig. 4). Zanclean strata are separated from Piacenzian/early Gelasian deposits by a Mid-Pliocene Unconformity (MPCU), while the latter deposits are separated from a late Gelasian/Calabrian interval by an early Pleistocene Unconformity (EPSU). Both the MPCU and the EPSU are related to tectonic movements along the main NW-striking fault zones bounding the Crotona Basin (Zecchin et al., 2020).

3. Data and methods

The studied dataset comprises 2D multichannel seismic reflection profiles and borehole data provided by ENI Natural Resources (Figs. 5, 6 and 7). The interpreted 2D seismic dataset spans the proximal offshore sector of the Crotona Basin, and images the continental shelf and slope (Fig. 5, 6 and 8). Borehole and seismic interpretations were carried out in the time domain using Schlumberger's Petrel[®]. Seismic data interpretation included the recognition of key seismic reflectors, which generally correlate with lithological changes and unconformities in borehole data. The recognition of key horizons was based on the identification of seismic reflection terminations, changes in seismic facies and seismic-borehole ties.

The interpretation of continental red beds and source rocks in Mesozoic carbonates was based on the fact that the organic-rich shales usually act as detachment layers for thrust faults and broader folds (Waldron *et al.*, 2011). In the study area, faults and folds were recognised both above and below putative detachment zones, within which seismic reflectors show significant horizontal shortening and deformation (Figs. 3 and 4).

Schlumberger's PetroMod[®] was used to compute 1D burial/maturation plots for exploration boreholes and pseudo-wells in the study area. Model inputs such as lithology and the ages of stratigraphic units were derived from the Federica 1 and Lulù 1 boreholes, while palaeowater depths were assigned on the basis of the palaeogeographic evolution illustrated by Zecchin *et al.* (2020). For those units not penetrated by exploration boreholes, lithologies were derived from the literature documenting the sedimentary successions of the Ionian region (Critelli, 1999). The associated palaeowater depths assumed in the models were assigned on the basis of the lithologies drilled by the exploration boreholes. Heat-flow values (mW/m^2) for the Croton Basin were computed after considering the main lithologies in each stratigraphic interval and sea-water temperatures ($^{\circ}\text{C}$) using the default data provided by PetroMod[®] (Wygrala, 1989). Average values of input data are shown in table 1.

At the location of the Federica 1 borehole, the calibration between seismic and borehole data was based on the formula $time = thickness(m) * 2 / velocity(m/s)$. Where strata were not penetrated by boreholes, e.g. the Mesozoic rift succession, unit thickness was estimated after depth-converting the seismic data (see Table 2 for velocities). After reconstructing the structural evolution of the study area in the context of the Mediterranean Sea's evolution, we linked structural-stratigraphic interpretations to basin maturation models.

4. Results

4.1. Seismic stratigraphy

Seventeen seismic sequences were interpreted in this work and correlated with the regional lithostratigraphic framework in Critelli (1999) and Zecchin *et al.* (2020). Unit U1 pre-dates continental rifting, Units U2 and U3 correlate with late continental rifting and ocean spreading, while units U4 and U5 relate to Oceanic Anoxic Events and Alpine orogenesis, respectively. Units U6 to U11 are associated with Alpine orogenesis, while units U12 to U17 represent the Croton Basin fill (Figs. 3 and 4; Table 1). Locally, Units U12 and U13 comprise known reservoir intervals. Units U13 to U17 are part of a remobilised interval in which a large mass-transport complex is observed (Zecchin *et al.*, 2018; Mangano *et al.*, 2020).

4.1.1 Mesozoic units

Mesozoic strata are subdivided in units U1 to U5, which comprise transparent to high-amplitude, discontinuous and folded seismic reflections crossed by faults in the RSFZ (Figs. 5 and 6). The interpretation of these units was based on literature (Critelli *et al.* 1999), according to which the Mesozoic sedimentary succession of the Ionian Sea consists of Triassic organic-rich redbeds, overlain by very thick Early to Late Jurassic Carbonate platforms with intercalated Aptian/Cenomanian organic-rich shaley/marly thin intervals. The interpretation of organic-rich intervals was based on the fact that these types of rocks act as detachment layer for thrust faults.

We correlated the Triassic organic-rich red beds with U2, and the up to ~1000 m thick Early Jurassic to Late Cretaceous carbonates with units U3 and U5. In between U3 and U5, organic-rich shaley layers (Aptian/Cenomanian) occur in unit U4 (Zuffa *et al.*, 1980; Santantonio and Teale, 1987) (Figs. 3, 5 and 6).

4.1.2 Paleogene units

Paleogene strata comprise units U6, U7 and U8, intervals with transparent to high amplitude, discontinuous reflections with anticlinal folds (Figs 5 and 6). Based on the Federica 1 borehole, the three units are correlated with the Flysch di Albidona (late Paleocene-Late Eocene), which documents the initial phases of the Alpine and Apennine orogeneses (Fig. 3, Table 2).

4.1.3 Latest Paleogene (Oligocene) to Miocene units

Latest Paleogene (Oligocene)-Miocene strata include units U9 to U14, which are characterised by their low- to high-amplitude, folded and discontinuous seismic reflections (Figs. 5 and 6). Based on the Federica 1 and Lulù 1 boreholes, these units are correlated with the mixed siliciclastic and carbonate deposits of the Stilo Formation (Oligocene/Burdigalian) in unit U9, the epipelagic sediments of the Fedra Formation (Langhian) in units U10 and U11, the fan-delta conglomerates and sandstones of the San Nicola Formation (Serravallian; Zecchin *et al.*, 2020) in unit U12, the siltstone-dominated succession with sandy and gravelly layers of the Ponda Group (Tortonian; Zecchin *et al.*, 2020) in U13, and the Messinian diatomites, halite, resedimented evaporites, limestones, siliciclastic sandstones and conglomerates in unit U14 (Fig. 4). The Serravallian San Nicola Formation (U12) and the intercalated sands of the Tortonian Ponda Group (U13), constitute proven reservoir intervals in the Crotona Basin (Roveri *et al.*, 1992). The Messinian unit U14 is also part of large mass-transport-complex developing in the Crotona Basin since the Zanclean (Zecchin *et al.*, 2018; Mangano *et al.*, 2020; 2021; 2022b).

4.1.4 Pliocene-Quaternary units

Pliocene-Quaternary strata comprise units U15, U16 and U17, which are made up of low- to high-amplitude, folded and discontinuous seismic reflections, locally with a fan geometry (Figs. 5 and 6). Based on the Federica 1 and Lulù 1 boreholes, they correlate with the shelf to slope claystones of the Cavalieri Marl (Zanclean) and with the Cutro Clay (Piacenzian to Holocene; Zecchin *et al.*, 2020). These units were deposited during the oceanisation of the Vavilov and Marsili sub-basins in the Tyrrhenian backarc area. Towards the basin shoulder, U15, U16 and U17 are part of the large mass-transport-complex that created the so-called Crotona Swell (Zecchin *et al.*, 2018; Mangano *et al.*, 2020; 2021; 2022b) (Figs 5, 6 and 8).

4.2. The Rossano-San Nicola Fault Zone (RSFZ)

The NW-striking RSFZ intersects the NE boundary of the Crotona Basin and is part of a series of strike-slip faults generated due to the SE migration of the Calabrian Accretionary Wedge since the Middle Miocene (Muto *et al.*, 2014) (Figs. 1 and 8). The RSFZ consists of multiple faults offsetting all seismic-stratigraphic units interpreted in this work (Figs. 5 and 6). These faults form a positive flower structure and deform the Upper Miocene Unconformity (UMU), giving rise to its anticlinal geometry (Fig. 6). The northern branches of the flower structure tilted the Aptian to Oligocene units U4 to U9 towards the S, whereas units U10 to U17 reveal considerable thickness changes. Important thickening can be observed in the early Langhian unit U10, which has a fan geometry (Fig. 6).

Significant differences are observed along a WSW-ENE direction when comparing the deformation styles of distinct units (Fig. 6). The deeper faults, interpreted as positive flower structures, propagate upwards from unit U1 to terminate at the UMU. A detachment zone occurs between shaley and uppermost Triassic/Lower Jurassic limestone intervals in units U2 and U3 (Figs. 5 and 6). Secondary detachments cross similar lithologies in

Aptian/Cenomanian and Late Cretaceous units U4 and U5. In contrast, some of the shallowest faults in the study area offset the Zanclean and younger units U15 to U17, linking to the lower tier of faults terminating near the UMU (Fig. 5).

4.3 Basin Modelling (*burial and maturation models*)

The burial and thermal histories for two (2) exploration boreholes and three (3) pseudo-wells, partly coincident with industry boreholes drilled in the eastern and south-eastern offshore sector of the Crotona Basin, are shown in Figures 9 and 10. The Lulù 1 borehole (Fig. 6) and Pseudo-well 1 (Fig. 5) intersect two distinct anticlinal folds below the large mass-transport complex identified in the study area. The Federica 1 borehole is located on a structural high of inferred Messinian age, as documented by the direct contact between Zanclean and Langhian strata observed in seismic data (Fig. 5). Pseudo-well 2 lies on a small-scale depocenter of inferred Zanclean age (Fig. 5). Pseudo-well 3 crosses the eroded top of an anticlinal fold of inferred Tortonian age which, in turn, is sealed by siltstone-rich Tortonian to Pleistocene strata (Fig. 6).

The study area records alternating episodes of subsidence and tectonic uplift since the Early Mesozoic (Figs. 9 and 10). Important sedimentation took place in the Early Jurassic and Late Cretaceous, as documented by the 1D burial model for the vertical profile passing along the Federica 1 borehole (Fig. 9a). Tectonic plate reorganisation in the Central Mediterranean Sea (Stampfli and Borel 2002), major climatic and sea-level changes (Jenkyns *et al.* 1999), resulted in the deposition of relative thick carbonates. As a result, unit U2 reached the gas generation window during the Late Cretaceous (Fig. 9a). Near the Federica 1 borehole, Lower Jurassic-Upper Cretaceous carbonates reach a thickness of 2000 m (Fig. 9a).

Important sedimentation continued in the study area through the Paleogene with the accumulation of more than 2000 m of siltstones with intercalated sandy layers (Flysch di Albidona). These were followed by the deposition of ~1200 m of terrigenous clastic sediments (Stilo Formation) during the Oligocene and Early Miocene (Pseudo-well 3, Fig. 9c). However, at the location of Pseudo-well 3, the gas generation window was only reached by unit U2 in the Early Pliocene (Fig. 9c).

Near the Federica 1 borehole, Pliocene strata do not exceed 400 m in thickness (Fig. 9a). The presence of an evolving structural high hindered the generation of accommodation space for new sediment (Fig. 5). In addition, Langhian subsidence and deposition are markedly distinct when comparing the Federica 1 and Lulù 1 boreholes (Fig. 9d). Approximately 1800 m of Langhian strata were deposited at Lulù 1 as a result of transpressional faulting, whereas Federica 1 only shows very thin sediments of the same age. Source rocks at Lulù 1 entered the gas window in the Langhian and expelled gas until the present day. However, gas shows have not been found at this borehole location (Fig. 6).

Other important episodes of sedimentation are documented at Pseudo-well 2 (Fig. 9b). Here, approximately 2000 m of siltstones and claystones of the Cavalieri Marl and Cutro Clay were accumulated in the more distal sectors of the study area. Inference from seismic profiles support the presence of Zanclean tectonics, which controlled the development of a tectonic trough and promoted the deposition of considerable volumes of pelagic strata near Pseudo-well 2 (Fig. 5). Simultaneously, the portions of unit U2 lying below unit U15 entered the gas window during the Zanclean, remaining there until the present day (Fig. 9b).

In a more proximal (landward) position, burial plots confirm that the siltstones and claystone of the Cavalieri Marl and Cutro Clay, when considered together with the Messinian evaporites, form a ~ 1800 m thick succession at Pseudo-well 1 (Fig. 10). Seismic profiles show this interval as part of the distal compressional domain of a large mass-transport

complex, which overthrust older units after the mid-Pliocene contractional/transpressional event (Zecchin *et al.*, 2018; Mangano *et al.* 2020; Mangano *et al.*, 2021) (Fig. 5). It is also worth mentioning that unit U2 recorded elevated heat flow (62 mW/m^2) at the onset of mass-transport deposition (Fig. 9d).

Tectonic uplift and erosion affected the whole of the study area during the Paleocene, and around the Eocene/Oligocene boundary, in association with Mesoalpine tectonics and Apennine orogenesis (Federica 1, Fig. 9a). Minor tectonic uplift took place during the Langhian, Serravallian and Tortonian, as documented by the burial history plots computed for the Federica 1 and Lulù 1 boreholes (Figs. 9a, d). An important phase of uplift occurred during the Messinian alongside tectonic collision amongst the Calabrian Arc and adjacent tectonic plates (Federica 1, Pseudo-Well 2, Lulù 1; Figs. 9a, b, d). In a more landward position, the decrease in water depth and the ca. 1700 m sediments deposited during the mid-Pliocene are associated with the emplacement of a large mass-transport complex (Figs. 5 and 10).

5. Local tectonic controls on source rock maturation and burial history

The new tectono-stratigraphic framework presented in this paper emphasises the tectonic control exerted by the RSFZ on the subsidence/burial and maturity history of the offshore eastern sector of the Crotona Basin. Most of commercial gas pools in this area are associated with the culmination of a compressional structure that was reactivated during the Pliocene (Roveri *et al.*, 1992) and near Pseudo-well 1 (Fig. 5). In contrast, no gas shows have been found at Federica 1 and Lulù 1.

In this work, the integration of 2D seismic data and 1D forward models reveal that local tectonics exerted a positive impact on the petroleum systems of the Crotona Basin. Anticlinal

traps at the level of the Tortonian reservoirs, plus Messinian-Pleistocene evaporites and siltstone seal intervals, are part of the compressional domain of a mass-transport complex triggered by RSFZ-related, Mid-Pliocene contraction/transpression (Fig. 5). The emplacement of more than 1000 m of mass-wasted strata during the Pliocene blanketed the known source-rock intervals and kept them in the gas window until the present day (Fig. 10). In contrast, local tectonics near gas-producing boreholes had a negative impact on trap development. Although maturity conditions are still present near the Federica 1 and Lulù 1 boreholes (Fig 9a, d). The significant contractional/transpressional tectonics recorded from Late Cretaceous to the late Paleogene, and later Neogene RSFZ-linked tectonics, led to the development of dense fault families that acted as fluid escape pathways.

6. Discussion

6.1 Geotectonic significance of interpreted seismic-stratigraphic units

Pangea's fragmentation during the Triassic is documented, throughout Europe, by the widespread deposition of continental red beds (Perri *et al.*, 2013). The latter are found along the tectonic nappes that form the Calabrian Arc, at the base of the Meso-Cenozoic Sila and Stilo units, and comprise red-purple mudrocks and silty clays (Perrone *et al.*, 2006). Given that detachment faults are facilitated along shale-prone units (Morley *et al.*, 2018), we therefore correlate unit U2 with Triassic/Jurassic organic-rich red beds that lie above U1 in the study area (Figs. 5 and 6). Unit U3 reflects a period of relative tectonic quiescence. In contrast, unit U4 is folded due to detachments faults formed along shaley layers in unit U2 (Morley *et al.*, 2018).

The top of unit U5 (Horizon 5) is truncated and locally sealed by unit U6. Unit U5 is associated with Late Cretaceous subduction of the Neotethys based on the published

stratigraphic frameworks (Zuffa *et al.*, 1980; Santantonio and Teale, 1987; Critelli, 1999) and Jenkins, 1999) (Fig. 3). Above U5, the Federica 1 borehole records the presence of middle Eocene to Oligocene strata to a thickness of ~ 2000 m (Fig. 7). We infer that the Late Cretaceous tectonic convergence led to the uplift of the study area and prevented the accumulation of Paleocene to Lower Eocene strata corresponding to U8.

Unit U7 correlates with the upper part of the “Flysch di Albidona” (Middle Eocene). At this time, the Mediterranean region experienced compressional tectonics in both the African and Eurasian plates under Alpine Orogenesis (Stampfli, 2005) (Fig. 3). Several unconformities record discrete tectonic phases in the study area; the Upper Messinian Unconformity - UMU (Horizon 14 in Figs. 5 and 6), for instance, is considered to result from the temporary collision, and coupling, of the NE part of the Calabrian-Peloritanian domain with the Apulian margin at 5.42 Ma. It is also associated with tectonic convergence between the Apulian platform and western Greece (Massari and Prosser, 2013).

Pliocene-Quaternary units record a similar tectono-stratigraphic setting associated with Tyrrhenian back-arc extension and Calabrian Arc compression. Unit U15 (Cavallieri Marl) was accumulated during the Zanclean, relating to the ocean spreading phase of the Vavilov sub-basin in the Tyrrhenian Sea, which probably ended at ca. 2.6 Ma (Zecchin *et al.* 2020). Its top boundary, the mid-Pliocene Unconformity (MPCU, or Horizon 15), correlates with a compressional event involving the Calabrian Arc and continental crust of the Apulian margin (Van Dijk, 1991) (Figs. 5 and 6). It was also synchronous with the temporary interruption, or slowdown, of ocean spreading in the Tyrrhenian back-arc region at ca. 3.6 Ma, with corresponding Calabrian Arc migration (Zecchin *et al.*, 2020). This compressional event is correlated with the final stage of tectonic convergence between Apulia and NW Greece (Massari and Prosser 2013), suggesting that the Apennines, northern Calabria, and the external NW parts of the Hellenides were developing concomitantly at this time and

migrating towards Apulia (Chizzini *et al.*, 2022). In contrast, Horizon 16 correlates with the so-called Mid-Pleistocene unconformity (ESPU), which may be linked to the final collision between the North Calabrian Accretionary Wedge and the Apulian plate. The end of oceanisation in the Vavilov Basin is recorded at ca. 2.4 Ma (Zecchin *et al.*, 2012; 2020).

The youngest strata in the study area (unit U17) were deposited while the Marsili sub-basin was developing in the Tyrrhenian backarc area at ca. 2.1 Ma (Massari and Prosser, 2013). This sub-basin results from active trench rollback, back-arc extension and crustal rotation (Mattei *et al.*, 2007).

6.2. Tectono-stratigraphic evolution of the Crotona Basin

The data in this work highlight the effect of the RSFZ on the deformation and uplift of particular sectors of the Crotona Basin. This effect is best recorded by the development of several unconformities from the Early Miocene onwards (Figs 5 and 6). Compressional and transpressional tectonic pulses alternated in the Crotona Basin with periods of extension and basin subsidence. This is expected under a setting dominated by Apennine orogenesis, responding to tectonic convergence between the African and Eurasian plates (Stampfli, 2005), and by successive episodes of convergence between the Calabrian Arc, and adjacent tectonic (micro)plates, in the context of active rollback and subduction of the Ionian lithosphere below the Arc itself (Zecchin *et al.*, 2020).

The NW-striking RSFZ shows a complex geometry, comprising a lower positive flower structure offsetting Mesozoic to Tortonian units, and two distinct transtensional faults in Zanclean to Holocene strata (Figs. 5 and 6). These may stem from reactivated (i.e., older) transpressional structures. Indeed, compressional/transpressional structures and related unconformities are observed inside the Mesozoic to Oligocene/Burdigalian units U1 to U9 (Figs. 5 and 6). Their development may be a result of subduction of the African plate beneath

the Neotethys during the Late Cretaceous, and Apulia-Adria beneath Iberia during the Eocene-Oligocene (Stampfli, 2005; Stampfli *et al.*, 2009).

In the published literature, the RSFZ is considered to have developed since the Early Miocene as a consequence of tectonic separation between Calabria and the Sardinia Block, and simultaneous opening of the Tyrrhenian Sea (Tripodi *et al.*, 2018). Following Early Miocene transtension, a major compressional event occurred in the Langhian, as documented by the Early Langhian (ELU) and Middle Langhian (MLU) unconformities. These unconformities are better developed near the positive flower structure that dominates the southern part of the study area, which tilted the Aptian to Burdigalian units U4 to U9 (Fig. 6). At the location of Pseudo-well 3, structural tilting occurring at this time generated potential gas stratigraphic traps; the siliciclastic and carbonate platform deposits of the Oligocene to Burdigalian unit U9 form an anticlinal limb that is unconformably sealed by the siltstone-dominated Plio-Pleistocene succession (Fig. 6). This positive flower structure also led to the development of a small-scale depocenter where reflectors of the Langhian unit U10 thicken towards the basin depocenter, terminating against the left-hand fault branch of the flower structure itself (Fig. 6). We interpret this contractional/transpressional tectonic regime to have been associated with prolonged convergence between Africa and Eurasia, under a setting dominated by eastward roll-back of the Adria plate beneath the Apennine Range, induced by slab-pull or relative eastward mantle flow during the Early Miocene (Doglioni *et al.*, 1991).

Extensional/transensional tectonics is recorded in the study area during the Serravallian-Early Tortonian and led to the generation of the Crotona Basin (Massari and Prosser, 2013). It was accompanied by short-term episodes of RSFZ-related compressional/transpressional tectonics, resulting in the development of Serravallian (SU) and Tortonian (TU) unconformities. The presence of such unconformities highlights the formation, in the Middle to Late Miocene, of an anticline controlled by the positive flower structure that is the RSFZ

(Fig. 6). Along a WSW transect, the TU abruptly dips to the WSW, while the overlying unit U13 (Tortonian) thickens towards the basin shoulder (Figs. 5 and 6). The Middle to Late Miocene extensional/transensional phases that led to the opening of the Crotone Basin are also associated with tectonic separation between Calabria and the Sardinian Block (Massari and Prosser, 2013); however, the driving mechanisms leading to the formation of the SU and the TU are still poorly understood.

Contractional/transensional tectonic phases persisted during the late Messinian, resulting in the formation of the UMU (Massari and Prosser, 2013). This unconformity defines two prominent structural highs near fault segments in the RSFZ, under a setting dominated by subaerial exposure, as documented by the absence of Messinian deposits near this structure (Figs 5 and 6). Although these two areas comprise thick Oligocene to Tortonian siliciclastics, and carbonate sediments sealed by Plio-Pleistocene siltstone-dominated deposits, no gas shows have been found by exploration boreholes. Late Messinian contractional/transensional reactivation of the RSFZ may have been related to incipient collision and temporary coupling between the NE part of the Calabrian Arc and the Apulian margin. As mentioned in Section 6.1, this tectonic event seems to be closely related to the collision of western Greece with Apulia (Massari and Prosser, 2013).

Late Messinian contractional/transensional tectonics was followed by an extensional/transensional episode associated with the RSFZ. This episode is highlighted by the presence of normal faults in the RSFZ, which led to the development of local Zanclean divergent reflections of unit U15 in the distal part of the WSW-ENE profile in Fig. 5. Such extensional/transensional structures probably used older inherited faults, matching the well-known Zanclean phase of subsidence related to back-arc extension in the Tyrrhenian Sea. It ultimately led to the opening of the Vavilov sub-basin (Chiarabba *et al.*, 2008).

After Zanclean subsidence, the RSFZ experienced a phase of contractional/transpressional tectonics, which led to the formation of a Mid-Pliocene Unconformity - MPCU (Massari and Prosser, 2013). Seismic profiles document that the MPCU bounds a noticeable structural high along a WSW direction, whose development seems to be associated with the reverse fault segments that constitute the RSFZ (Fig. 5). This same mid-Pliocene contractional/transpressional event contributed to the accumulation of reservoir and seal units in the northern sector of the Croton Basin. According to Mangano et al. (2021), such compressional/transpressional tectonic episode resulted in the accumulation of a large mass-transport complex, resulting in the so-called Croton Swell (Figs. 5 and 8). The sedimentary succession of this Croton Swell includes sandstone and siltstone-dominated Tortonian reservoirs in unit U13, sealed by the evaporite- and mudstone-dominated Messinian and Plio-Pleistocene units U14 to U17. The Croton Swell also lies above the Serravallian reservoirs in unit U12. Such an interpretation contrasts with the idea of Roveri et al. (1992), who considered the Tortonian and Serravallian reservoir intervals to be sealed by a Pliocene compressional structure recognised along the Apennine Orogen. According to our interpretation, the Tortonian and Serravallian reservoirs are sealed by a large mass-transport complex only locally developed in the Croton Basin (Fig. 5).

At a regional scale, the late Zanclean/Early Piacenzian contractional/transpressional tectonic event is associated with the final collision - involving Apulia, the southern Apennines and the Calabrian Arc - with NW Greece at ca. 3.6 Ma. Such a collision caused the temporary halt of the Calabrian Arc's SE-ward migration and an interruption (or slowdown) of ocean spreading in the Vavilov sub-basin (Zecchin *et al.*, 2020).

After the late Zanclean/Early Piacenzian contractional/transpressional tectonic event, the Croton Basin recorded alternating phases of subsidence and basin inversion. Seismic profiles show that the RSFZ was active during the Piacenzian/earliest Gelasian and from the

middle Gelasian onwards. The development of divergent seismic reflections in Piacenzian/earliest Gelasian and middle Gelasian strata appears to have been governed by discrete fault segments that form the RSFZ itself (Fig. 5). The driving mechanism of such an extensional/transensional tectonic regime can be correlated with the youngest spreading of the Vavilov back-arc sub-basin, which ended at ca. 2.6 Ma (Zecchin et al., 2020), and with the opening of the Marsili Basin initiated at ca. 2.1, simultaneously with a clockwise rotation of ca. 20° and SE-ward migration of the Calabrian Arc (Massari and Prosser, 2013). In contrast, the deformational event at ca. 2.4 that generated the Early Pleistocene Unconformity (EPSU) is not clear in seismic data, as this stratigraphic marker is conformable in the study area (Figs. 5 and 6).

6.3. Burial and thermal histories of the Crotona Basin

The alternating influence of Pliocene extensional/transensional and contractional/transpressional tectonics on the RSFZ is considered a key element in the deepening and maturity of source rock intervals in the Crotona Basin. Our 1D burial plots indicate that the greatest burial depths of Triassic/Lower Jurassic (up to 9000 m) and Aptian/Cenomanian source rocks occurred at the end of the Zanclean and just after the Early Pliocene (e.g., Pseudo-wells 1 and 2, Figs 9 and 10). Zanclean extensional/transensional tectonics led to the development of a tectonic trough in the distal parts of the study area, in which up to 2000 m of sediments were deposited, whereas the Mid-Pliocene contractional/transpressional event led to the emplacement of a ~ 2000 m thick mass-transport complex in a relatively proximal position in the basin (Fig. 5). Seismic profiles show that the divergent reflections in unit U15 (Zanclean) are associated with RSFZ-related normal faults, whilst the emplacement of the large mass-transport complex was triggered by contractional/transpressional activity in the RSFZ (Mangano *et al.*, 2021) (Fig. 5). The

resulting sediment loading due to the emplacement of this complex correlates with a maturity maximum in Triassic/Lower Jurassic source rocks (Fig. 10). This means that while the area in which the large mass-transport complex is recognised represents a proven prolific gas province since 1970 (Roveri *et al.*, 1992), the region surrounding the Zanclean tectonic trough may not be prospective in terms of gas because of the presence of a significant number of faults (Fig. 5).

Other phases of subsidence and associated thermal maturity have occurred since the Early Miocene near the Lulù 1 borehole (Fig. 9d). The contractional/transpressional phases experienced by the RSFZ facilitated high sedimentation rates in the order of 2500 m in ~ 2.0 Myrs in the basin depocenter and were followed by progressive sedimentation and emplacement of large mass-transport deposits. The latter enhanced the burial of strata and kept putative source rocks in the gas window until the present day. Nevertheless, no gas shows were recorded by the Lulù 1 borehole.

The study area also recorded successive episodes of tectonic uplift during the Paleogene and the Miocene (Langhian - late Messinian), as highlighted by the 1D burial plots in Figs. 9 and 10. Correlations amongst our 1D forward models and seismic data reveal that both Early and Late Miocene tectonic uplift are linked to contractional/transpressional activity in the RSFZ. The youngest phase of uplift may be a consequence of the rollback of Adria's subducted slab beneath the Apennines, reactivating inherited Late Cretaceous to Paleogene tectonic structures.

Despite the repeated episodes of tectonic uplift experienced by the study area, gas generation are predicted to have continued from the Late Cretaceous, until the present day, at the Federica 1 borehole (Fig. 9a). This suggests the thickness of Cretaceous sediments to have been enough to mask the effects of uplift and erosion in terms of source rock maturity. Conversely, when considering Pseudo-well 3, an early Langhian paroxysmal phase of

tectonic uplift prevented the accumulation of Langhian to Serravallian sediments and cooled the source-rock intervals below (Figs. 5 and 9c). Paradoxically, the RSFZ-related uplift that resulted in the tilting of the Mesozoic to Paleogene succession near Pseudo-well 3 would not have had a negative impact on source-rock maturity, as these same source rocks reached the gas generation window during the Quaternary after the accumulation of a ~ 1000 m thick Plio-Pleistocene sedimentary cover.

7. Conclusions

This work shows how the activity of a large multi-phased strike-slip fault zone was able to control the burial and thermal maturity histories of the Croton Basin, as well as seal and trap development, under the geodynamic events that affected the central Mediterranean region. The main conclusions of this work are summarised as follows:

a) The RSFZ records alternating phases of extensional/transensional and contractional/transpressional tectonics during the Late Cenozoic, which controlled the evolution of depocentres, structural highs, and the emplacement of a large mass-transport complex. A phase of contractional/transpressional tectonics is inferred to have occurred during the Langhian, as evidenced by the tilting of Aptian to Burdigalian units U4 to U9 towards the S, concomitantly with the opening of a small depocenter with divergent reflections in unit U10 (Langhian). This promoted high sedimentation rates and favourable conditions for source-rock maturation in the SE sector of the Croton Basin, as documented by the ca. 2.0 s (TWT) thick units U10 and U11 (Langhian). This sector, however, is not a potential gas exploration site, as proven by its dry boreholes. Further fluid expulsion occurred here during the Late Cretaceous and Zanclean with respect to the only gas-producing field in the basin. The RSFZ-related contractional/transpressional event controlled the development

of structural traps between tilted siliciclastic and carbonate deposits (Oligocene to Burdigalian) and the very thick siltstone-dominated Plio-Pleistocene sedimentary cover. This is also supported by Pseudo-well 3, which suggests that Triassic/Lower Jurassic source rocks entered the gas window in the Pliocene, until the present day, just east of a gas-producing field.

b) Other contractional/transpressional episodes took place during the Serravallian, Tortonian, Late Messinian and mid-Pliocene as highlighted by the development of multiple unconformities on evolving structural highs. Intense extensional/transensional tectonics is documented during the Zanclean by the development of syn-depositional growth affecting unit U15 (Zanclean) towards the distal parts of the Croton Basin.

c) The RSFZ-related Zanclean extensional/transensional tectonics, plus the widespread accumulation of a large mass-transport complex derived from a Mid-Pliocene contractional/compressional event, deepened the Croton Basin and, therefore, enhanced the thermal maturity of Triassic/Jurassic source rocks in its distal sector. The emplacement of the large mass-transport complex is considered the main control factor for gas generation in the gas-producing area of the Croton Basin. This is documented by the maximum depth of 9000 m reached by Triassic/Lower Jurassic (U2) and Aptian/Cenomanian (U4) source rocks below this mass-transport complex. In contrast, the Zanclean extensional/transensional tectonic event did not create favourable traps, as the presence of faults suggest an increased risk of fluid losses in the basin.

d) Nevertheless, the gas generation window was reached in the SE sector of the Crotona Basin as a consequence of the deposition of thick carbonate and Plio-Pleistocene sedimentary covers. The Federica 1 borehole and Pseudo-well 3 suggest the Triassic/Lower Jurassic source rocks (U2) to have entered the gas window during the Late Cretaceous, concomitantly with the deposition of up to 2000 m thick carbonates in unit U5. The gas window was also reached in the Zanclean as a result of the deposition of more than 1000 m of Plio-Pleistocene strata in units U15 to U17.

Funding

No funding was received for this work.

Declaration of interests

The authors declare that they have no known competing financial interests or personal relationships that could have appeared to influence the work reported in this paper.

Acknowledgments

Geophysical and geological data were provided by ENI Natural Resources. We also acknowledge Schlumberger (for Petrel® and Petromod®) for providing academic licences to Cardiff's 3D Seismic Lab.

REFERENCES

Angrand, P., Mounthereau, F., Masini, E. and Asti, R. 2020. A reconstruction of Iberia accounting for Western Tethys–North Atlantic kinematics since the late-Permian–Triassic.

Solid Earth 11, 1313–1332. <https://doi.org/10.5194/se-11-1313-2020>

Alves, T., Fetter, M., Busby, C., Gontijo, R., Cunha, T.A. and Mattos, N.H. 2020. A tectono-stratigraphic review of continental breakup on intraplate continental margins and its impact on resultant hydrocarbon systems. *Marine and Petroleum Geology* 117, 104341. <https://doi.org/10.1016/j.marpetgeo.2020.104341>.

Alves, T.M. 2010. 3D Seismic examples of differential compaction in mass-transport deposits and their effect on post-failure strata. *Mar. Geol.* 271, 212-224.

Alves, T.M. 2015. Submarine slide blocks and associated soft-sediment deformation in deep-water basins: a review. *Mar. Petroleum Geol.* 67, 262-285.

Catalano, R., Doglioni, C. and Merlini, S. 2001. On the Mesozoic Ionian basin. *Geophysical Journal International*, 144(1), 49-64.

Channell, J. E. T., Muttoni, G. and Kent, D. V. 2022. Adria in Mediterranean paleogeography, the origin of the Ionian Sea, and Permo-Triassic configurations of Pangea. *Earth-Science Reviews*, 230, 104045.

Chiarabba, C., De Gori, P. and Speranza, F. 2008. The southern Tyrrhenian subduction zone: deep geometry, magmatism and Plio-Pleistocene evolution. *Earth and Planetary Science Letters*, 268(3-4), 408-423.

Chizzini, N., Artoni, A., Torelli, L., Basso, J., Polonia, A., Gasperini, L. 2022. Tectono-stratigraphic evolution of the offshore Apulian Swell, a continental sliver between two converging orogens (Northern Ionian Sea, Central Mediterranean) *Tectonophysics*, 839, Article 229544, [10.1016/j.tecto.2022.229544](https://doi.org/10.1016/j.tecto.2022.229544). Critelli, S. 1993. Sandstone detrital modes in

the Paleogene Liguride Complex, accretionary wedge of the southern Apennines (Italy). *Journal of Sedimentary Research*, 63(3), 464-476.

Critelli, S. 1999. The interplay of lithospheric flexure and thrust accommodation in forming stratigraphic sequences in the southern Apennines foreland basin system, Italy. *Rendiconti Lincei* 10(4), 257-326.

Critelli, S. 2018. Provenance of Mesozoic to Cenozoic Circum-Mediterranean sandstones in relation to tectonic setting. *Earth-Science Reviews* 185, 624-648.

Critelli, S. and Martin-Martin, M. 2022. Provenance, Paleogeographic and paleotectonic interpretations of Oligocene-Lower Miocene sandstones of the western-central Mediterranean region: a review. In: "The evolution of the Tethyan orogenic belt and, related mantle dynamics and ore deposits". *Journal of Asian Earth Sciences Special Issue X8*, 100124 [10.1016/j.jaesx.2022.100124].

Critelli, S., Muto, F. and Tripodi, V. 2016. Note illustrative della Carta Geologica D'Italia alla scala 1:50.000 foglio 590 Taurianova. ISPRA (Istituto Superiore per la Protezione e la Ricerca Ambientale), *Servizio Geologico d'Italia*, Progetto CARG.

Csontos, L. and Vörös, A. 2004. Mesozoic plate tectonic reconstruction of the Carpathian region. *Palaeogeography, Palaeoclimatology, Palaeoecology*, 210(1), 1-56.

Doglioni, C. 1991. A proposal of kinematic modelling for-dipping subductions. Possible applications to the Tyrrhenian–Apennines system. *Terra Nova* 3, 423–434.

El Hassan, W. M. and El Nadi, A. H. H. 2015. Impact of inversion tectonics on hydrocarbon entrapment in the Baggara Basin, western Sudan. *Marine and Petroleum Geology*, 68, 492-497.

Espurt, N., Hippolyte, J. C., Saillard, M. and Bellier, O. 2012. Geometry and kinematic evolution of a long-living foreland structure inferred from field data and cross section balancing, the Sainte-Victoire System, Provence, France. *Tectonics*, 31(4).

Faccenna, C., Piromallo, C., Crespo-Blanc, A., Jolivet, L. and Rossetti, F. 2004. Lateral slab deformation and the origin of the western Mediterranean arcs. *Tectonics* 23, TC1012. <http://dx.doi.org/10.1029/2002TC001488>.

Feraud, G. 1990. ³⁹Ar-⁴⁰Ar analysis on basaltic lava series of Vavilov Basin, Tyrrhenian Sea (Ocean Drilling Program, Leg 107, holes 655B and 651A). In *Proc. Ocean Drill. Program Sci. Results* (Vol. 107, pp. 93-97).

Finetti, I. 1985. Structure and evolution of the central Mediterranean (Pelagian and Ionian Seas). *Geological evolution of the Mediterranean Basin*, 215-230.

Fraser, A.J. 2010. A regional overview of the exploration potential of the Middle East: a case study in the application of play fairway risk mapping techniques, Geological Society, London, Petroleum Geology Conference series. *Geological Society of London* 7 (1), 791–800.

Handy, M. R., Schmid, S. M., Bousquet, R., Kissling, E. and Bernoulli, D. 2010. Reconciling plate-tectonic reconstructions of Alpine Tethys with the geological–geophysical record of spreading and subduction in the Alps. *Earth-Science Reviews*, 102(3-4), 121-158.

Jenkyns, H. C. 1980. Cretaceous anoxic events: from continents to oceans. *Journal of the Geological Society*, 137(2), 171-188.

Jenkyns, H. C. 1999. Mesozoic anoxic events and palaeoclimate. *Zentralblatt für Geologie und Paläontologie*, 1997(7-9), 943-949.

Jolivet, L., Baudin, T., Calassou, S., Chevrot, S., Ford, M., Issautier, B., Lasseur, E., Masini, E., Manatschal, G., Mouthereau, F. and Thinon, I., 2021. Geodynamic evolution of a wide plate boundary in the Western Mediterranean, near-field versus far-field interactions. *BSGF-Earth Sciences Bulletin*, 192(1), p.48.

Kamberis, E., Kokinou, E., Koci, F., Lioni, K., Alves, T. M. and Velaj, T. 2022. Triassic evaporites and the structural architecture of the External Hellenides and Albanides (SE Europe): controls on the petroleum and geoenergy systems of Greece and Albania. *International Journal of Earth Sciences*, 111(3), 789-821.

Maerten, L., Legrand, X., Castagnac, C., Lefranc, M., Joonnekindt, J.-P, and Maerten, F. 2019. Fault-related fracture modeling in the complex tectonic environment of the Malay Basin, offshore Malaysia: An integrated 4D geomechanical approach. *Marine and Petroleum Geology* 105, 222-237.

Maffione, M., Hinsbergen, D.J.J., Gelder, G.I.N.O., Goes, F.C. and Morris, A. 2017. Kinematics of Late Cretaceous subduction initiation in the Neo-Tethys Ocean reconstructed from ophiolites of Turkey, Cyprus, and Syria. *J. Geophys. Res.: Solid Earth* 122, 3953e3976, 701.

Mangano, G., Ceramicola, S., Zecchin, M., Brancatelli, G. and Critelli, S., 2021. Geohazard-related geomorphic features in the Crotona-Spartivento Basin (Southern Italy): an expression of Calabrian Arc kinematics. *Offshore Med Energy Conference & Exhibition, Ravenna*. OMC-2021-167. <https://onepetro.org/OMCONF/proceedings-abstract/OMC21/All-OMC21/OMC-2021-167/473262>.

Mangano, G., Zecchin, M. and Civile, D. 2020. Large-scale gravity-driven phenomena in the Crotona Basin, southern Italy. *Marine and Petroleum Geology* 117, 104386.

- Marchant, R. H. and Stampfli, G. M. 1997. Subduction of continental crust in the Western Alps. *Tectonophysics*, 269(3-4), 217-235.
- Martín-Algarra, A., Solé de Porta, N., Maate, A., 1995. El Triásico del Maláguide-Gomáride (Formación Saladilla, Cordillera Bética Occidental y Rif Septentrional). Nuevos datos sobre su edad y significado palaeogeográfico. *Cuad. Geol. Ibérica* 19, 249–278.
- Massari, F. and Prosser, G. 2013. Late Cenozoic tectono-stratigraphic sequences of the Croton Basin: insights on the geodynamic history of the Calabrian arc and Tyrrhenian Sea. *Basin Research* 25(1), 26-51.
- Mauffret, A., Frizon de Lamotte, D., Lallemand, S., Gorini, C. and Maillard, A. 2004. E–W opening of the Algerian Basin (western Mediterranean). *Terra Nova*, 16(5), 257-264.
- Morley, C. K., Von Hagke, C., Hansberry, R., Collins, A., Kanitpanyacharoen, W. and King, R. 2018. Review of major shale-dominated detachment and thrust characteristics in the diagenetic zone: Part II, rock mechanics and microscopic scale. *Earth-Science Reviews*, 176, 19-50.
- Muto, F., Spina, V., Tripodi, V., Critelli, S. and Roda, C. 2014. Neogene tectonostratigraphic evolution of allochthonous terranes in the eastern Calabrian foreland (southern Italy). *Italian Journal of Geosciences*, 133(3), 455-473.
- Perri, F., Critelli, S., Martín-Algarra, A., Martín-Martín, M., Perrone, V., Mongelli, G. and Zattin, M., 2013. Triassic redbeds in the Malaguide Complex (Betic Cordillera — Spain): petrography, geochemistry, and geodynamic implications. *Earth-Sci. Rev.* 117, 1–28.
- Roveri, M., Bernasconi, A., Rossi, M. E., Visentin, C. and Spencer, A. M. 1992. Sedimentary evolution of the Luna Field area, Calabria, southern Italy. *Generation, Accumulation and Production of Europe's Hydrocarbons II: European Association of Petroleum Geoscientists, Special Publication*, 2, 217-224.

Rossetti F, Goffé B, Monié P, Faccenna C, Vignaroli G. 2004. Alpine orogenic P-T-t-deformation history of the Catena Costiera area and surrounding regions (Calabrian Arc, southern Italy): the nappe edifice of north Calabria revised with insights on the Tyrrhenian-Apennine system formation. *Tectonics* 23. DOI: 10.1029/2003TC001560.

Santantonio, M. and Teale, C. 1987. An example of the use of detrital episodes in elucidating complex basin histories: the Caloveto and Longobucco Groups of NE Calabria, S. Italy. *In Marine clastic sedimentology* (pp. 62-74). Springer, Dordrecht.

Saspiturry, N., Lahfid, A., Baudin, T., Guillou-Frottier, L., Razin, P., Issautier, B., Serrano, O., Le Bayon, B., Lagabrielle, Y. and Corre, B. 2020. Paleogeothermal gradients across an inverted hyperextended rift system: Example of the Mauléon Fossil Rift (Western Pyrenees). *Tectonics*, 39(10), e2020TC006206.

Schettino, A., Tassi, L. and Turco, E. 2010. Reply to comment by Cinthia Labails and Walter R. Roest on 'Breakup of Pangaea and plate kinematics of the central Atlantic and Atlas regions'. *Geophysical Journal International*, 183(1), 99-102.

Stampfli, G. M. and Borel, G. D. 2002. A plate tectonic model for the Paleozoic and Mesozoic constrained by dynamic plate boundaries and restored synthetic oceanic isochrons. *Earth and Planetary science letters*, 196(1-2), 17-33.

Stampfli, G. M. and Finetti, I. R. 2005. Plate tectonics of the Apulia-Adria microcontinents. *CROP Project-Deep Seismic explorations of the Central Mediterranean and Italy, Section*, 11, 747-766.

Stampfli, G. M. and Hochard, C. 2009. Plate tectonics of the Alpine realm. *Geological Society, London, Special Publications*, 327(1), 89-111.

- Sun, Q., Alves, T., Xie, X., He, J., Li, W. and Ni, X. 2017. Free gas accumulations in basal shear zones of mass-transport deposits (Pearl River Mouth Basin, South China Sea): An important geohazard on continental slope basins. *Marine and Petroleum Geology*, 81, 17-32.
- Tansi, C., Muto, F., Critelli, S. and Iovine, G. 2007. Neogene-Quaternary strike-slip tectonics in the central Calabrian Arc (southern Italy). *Journal of Geodynamics*, 43(3), 393-414.
- Tari, G., Arbouille, D., Schléder, Z. and Tóth, T. 2020. Inversion tectonics: a brief petroleum industry perspective. *Solid Earth*, 11(5), 1865-1889.
- Tripodi, V., Muto, F., Brutto, F., Perri, F. and Critelli, S. 2018. Neogene-Quaternary evolution of the forearc and backarc regions between the Serre and Aspromonte Massifs, Calabria (southern Italy). *Marine and Petroleum Geology* 95, 328-343.
[<https://doi.org/10.1016/j.marpetgeo.2018.03.028>].
- Van Dijk, J. P. 1991. Basin dynamics and sequence stratigraphy in the Calabrian Arc (Central Mediterranean); records and pathways of the Croton Basin. *Geologie en Mijnbouw* 70, 187-201.
- Van Dijk, J., Okkes, M., 1991. Neogene tectonostratigraphy and kinematics of Calabrian basins; implications for the geodynamics of the Central Mediterranean. *Tectonophysics*, 196(1-2), 23-60.
- Van Dijk, J. P., Bello, M., Brancaleoni, G. P., Cantarella, G., Costa, V., Frixia, A., Golfetto, F., Merlini, S., Riva, M., Torricelli, S., Toscano, C., Zerilli, A., 2000. A regional structural model for the northern sector of the Calabrian Arc (southern Italy). *Tectonophysics*, 324(4), 267-320.
- Van Hinsbergen, D. J., Torsvik, T. H., Schmid, S. M., Mañenco, L. C., Maffione, M., Vissers, R. L., Gürer, D. and Spakman, W. 2020. Orogenic architecture of the Mediterranean region

and kinematic reconstruction of its tectonic evolution since the Triassic. *Gondwana Research*, 81, 79-229.

Vergés J, Fernández M. 2012. Tethys-Atlantic interaction along the Iberia-Africa plate boundary: The Betic-Rif orogenic system. *Tectonophysics* 579: 144–172. DOI: 110.1016/j.tecto.2012.1008.1032

Vissers, R.L.M. and Meijer, P.Th. 2012. Mesozoic rotation of Iberia: Subduction in the Pyrenees? *Earth-Science Reviews* 110, 93-110.
<https://doi.org/10.1016/j.earscirev.2011.11.001>

Waldron, J. W. and Gagnon, J. F. 2011. Recognizing soft-sediment structures in deformed rocks of orogens. *Journal of Structural Geology*, 33(3), 271-279.

Wygrala, B.P. 1989. Integrated study of an oil field in the Southern Po Basin, Northern Italy. Ph.D. dissertation, University of Cologne, Germany. 328 pp.

Zecchin, M., Accaino, F., Ceramicola, S., Civile, D., Critelli, S., Da Lio, C., Mangano, G., Prosser, G., Teatini, P. and Tosi, L. 2018. The Croton Megalandslide, southern Italy: Architecture, timing and tectonic control. *Scientific reports* 8(1), 1-11.

Zecchin, M., Civile, D., Caffau, M., Critelli, S., Muto, F., Mangano, G. and Ceramicola, S. 2020. Sedimentary evolution of the Neogene-Quaternary Croton Basin (southern Italy) and relationships with large-scale tectonics: A sequence stratigraphic approach. *Marine and Petroleum Geology* 117, 104381.

Zecchin, M., Nalin, R. and Roda, C. 2004. Raised Pleistocene marine terraces of the Croton peninsula (Calabria, southern Italy): facies analysis and organization of their deposits. *Sedimentary geology* 172(1-2), 165-185.

Zhao, F., Alves, T. M., Li, W. and Wu, S. 2015. Recurrent slope failure enhancing source rock burial depth and seal unit competence in the Pearl River Mouth Basin, offshore South China Sea. *Tectonophysics*, 643, 1-7.

Zuffa, G. G., Gaudio, W. and Rovito, S. 1980. Detrital mode evolution of the rifted continental-margin Longobucco Sequence (Jurassic), Calabrian Arc, Italy. *Journal of Sedimentary Research*, 50(1), 51-61.

ACCEPTED MANUSCRIPT

Figure captions

Figure 1. a) Structural map of the Calabrian Arc, which is located between the southern Apennine chain and Maghrebides thrust belt (modified from Van Dijk and Okkes, 1991). The Croton Basin (red-colored square), part of the Calabrian Accretionary Wedge, is located on the Ionian side of the Arc and includes the Luna Field (blue-colored square). The Vavilov and the Marsili back-arc basins are located in the southern Tyrrhenian Sea. Also shown are NW-striking fault zones, including the RSFZ, segmenting the Calabrian Accretionary Wedge and Arc since the Miocene. b) NW-SE section across the Calabrian Arc (see the A-A' transect in Fig. 1a), displaying main structural elements (modified from Van Dijk et al., 2000). The Croton Basin, which constitutes the northern depocenter of the Croton-Spartivento Basin, is a forearc basin overlapping the Sila Massif.

Figure 2. Geodynamic reconstruction of the central Mediterranean region under Pangea continental break-up and the Alpine and Apennine orogeneses during: a) Late Triassic (Schmid et al., 2004), b) Late Jurassic (Schmid et al., 2004), c) Late Cretaceous (Stampfli and Finetti, 2005), d) Eocene (Stampfli and Hochard, 2009), e) Late Oligocene and Early Miocene (Chizzini et al., 2022), f) Middle/Late Miocene (Chizzini et al., 2022), g) Messinian (Chizzini et al., 2022), h) Pliocene (Chizzini et al., 2022), and i) the present-day (Chizzini et al., 2022). , RSFZ - Rossano-San Nicola Fault Zone.

Figure 3. Triassic to upper Langhian stratigraphic succession beneath the Mid-Miocene to Recent Croton Basin. The illustrated succession is based on data from the literature (Shlanger and Jenkyns, 1976; Jenkins, 1980; Zuffa *et al.*, 1980; Santantonio and Teale, 1987; Jenkins, 1999; Critelli, 1999; Critelli *et al.*, 2008; Critelli et al., 2016 – Foglio 590 Taurianova; Perri et al., 2013), which documents the widespread

presence of Triassic continental red beds, overlain by very thick Lower Jurassic to Upper Cretaceous carbonates with intercalated Aptian-Cenomanian shaley intervals. The Late Cretaceous to Late Langhian stratigraphy of the study area is reconstructed based on boreholes Federica 1 and Lulù 1 (see Fig. 8 for their locations). The stratigraphic succession below the Croton Basin is correlated with seismic-stratigraphic units U1 to U11 in the interpreted seismic data. LCU – Late Cretaceous Unconformity; EU – Eocene Unconformity; OU – Oligocene Unconformity; ELU – Early Langhian Unconformity; MLU - Mid-Langhian Unconformity.

Figure 4. Serravallian to Quaternary stratigraphic succession of the Croton Basin as interpreted from the published literature (Zecchin et al., 2020) and the Federica 1 and Lulù 1 boreholes (see Fig. 8 for their locations). The stratigraphic succession below the Croton Basin is correlated with

seismic-stratigraphic units U12 to U17 in the interpreted seismic data. SU - Serravallian Unconformity; TU – Tortonian Unconformity; ME – Base of Messinian; IMU – Intra-Messinian Unconformity; UMU – Upper Messinian Unconformity; MPCU – Mid-Pliocene Unconformity; EPSU – Early Pleistocene Unconformity.

Figure 5. a) Uninterpreted and b) interpreted 2D multichannel WSW-ENE seismic Profile 1 documenting the seismic-stratigraphic succession of the Calabrian Accretionary Wedge and Ionian Sea. The latter corresponds to the sediments deposited under the Neothethys rifting and the Africa - Eurasia collision, followed by the development of the Middle Miocene to Recent Croton Basin. A large mass-transport complex (MTC) corresponding to the Croton Swell is observed towards the WSW. The complex shows a WSW-dipping basal detachment surface (BDS) into which a reverse fault set terminates (green-colored segments). The MTC includes a Tortonian

reservoir unit U13, which is sealed by Messinian to recent units U14 to U17. The MTC also lies above Serravallian reservoirs in unit U12. Black-coloured segments indicate fault lineaments in the RSFZ. LCU – Late Cretaceous Unconformity; EU – Eocene Unconformity; OU – Oligocene Unconformity; ELU – Early Langhian Unconformity; SU – Serravallian Unconformity; TU – Tortonian Unconformity; UMU – Upper Messinian Unconformity; MPCU – Mid-Pliocene Unconformity; EPSU – Early Pleistocene Unconformity. The 2D multichannel seismic Profile 1 was provided by ENI Natural Resources. The exact location of Profile 1 is not shown on the map due to confidentiality rules imposed on the data.

Figure 6. a) Uninterpreted and b) Interpreted 2D multichannel N-S seismic Profile 2 documenting the seismic-stratigraphic succession of the Calabrian Arc and Ionian Sea. A large scale mass-transport complex (MTC) corresponding to the Crotona Swell

is observed towards the S. It shows a concave-up basal detachment surface (BDS) into which a N-dipping reverse fault set terminates (green-coloured segments). Black-coloured segments indicate fault lineaments, which form a positive flower structure belonging to the RSFZ. LCU – Late Cretaceous Unconformity; EU – Eocene Unconformity; OU – Oligocene Unconformity; ELU – Early Langhian Unconformity; SU – Serravallian Unconformity; TU – Tortonian Unconformity; UMU – Upper Messinian Unconformity; MPCU – Mid-Pliocene Unconformity; EPSU – Early Pleistocene Unconformity; MLU – Mid-Langhian Unconformity. The exact location of Profile 2 is not shown on the map due to confidentiality rules imposed on the data.

Figure 7. Available Federica 1 and Lulù 1 exploration boreholes located in the E and SE portions of the Crotona Basin, offshore Southern Italy. Original boreholes and their

locations are available at

<http://www.videpi.com/videpi/videpi.asp>

Figure 8. Digital Terrain Model (DTM) map under a UTM 33 (WGS84) projection highlighting the onshore and offshore parts of the Croton Basin (figure modified from Civile et al., 2022). The fault segments associated with the RSFZ as well as a mass-transport complex and related extensional faults are reported from this study and Massari and Prosser (2013), Zecchin et al. (2018, 2020) and Mangano et al. (2020). The locations of the Federica 1 and Lulù 1 boreholes are also shown in the figure.

Figure 9. Results of the burial history modelling from four locations in the Croton Basin: (a) Federica 1 borehole, (b) Pseudo-well 2, (c) Pseudo-well 3, (d) Lulù 1 borehole. At the location of Federica 1 (a) the Triassic/Early Jurassic unit U2 started generating gas in the upper Cretaceous, expelling it until the recent. (b) in Pseudo-well 2 the Triassic/Early Jurassic unit U2

entered the gas generation window during the Zanclean, remaining there until the present day. (c) at Pseudo-well 3 and (d) Lulù 1 borehole the Triassic/Early Jurassic unit U2 reached the gas generation window in the Early Miocene and Pleistocene. Significant sediment deposition during subsidence episodes can be identified in the study area during the (a) Late Cretaceous, (c) and (d) Paleogene, (d) Early Miocene and Zanclean. Heat-flow values were based on a crustal thickness of 16 km (see Table 1 for absolute values). The syn-rift event was considered to have happened from 180 Ma to 160 Ma, with stretching (beta factor) values of 3.00 for crust and mantle units.

Figure 10. PetroMod temperature models for Pseudo-well 1, which considers the effect of seal (U13 to U16) and reservoir (U11 and U12) intervals in the Luna Field. The Triassic/Early Jurassic unit U2 experienced its maximum depth in the Piacenzian and maintained the right conditions for gas maturation until the present day. Heat-flow

values were estimated based on a crustal thickness of 16 km. The syn-rift event was considered to have happened from 180 Ma to 160 Ma, with stretching (beta factor) values of 3.00 for crust and mantle units. The value of 3.00 has been used by default.

Table 1. Values and lithologies assigned to each seismic-stratigraphic unit in order to simulate the burial/maturity history of the Croton Basin.

Table 2. Information concerning the thickness, velocity, internal character and geometry for each seismic-stratigraphic unit considered in this work. The table also provides information on the correlations undertaken amongst lithology, main geological events and the inferred seismic-stratigraphic units separated by interpreted seismic horizons, or unconformities.

Figure 1

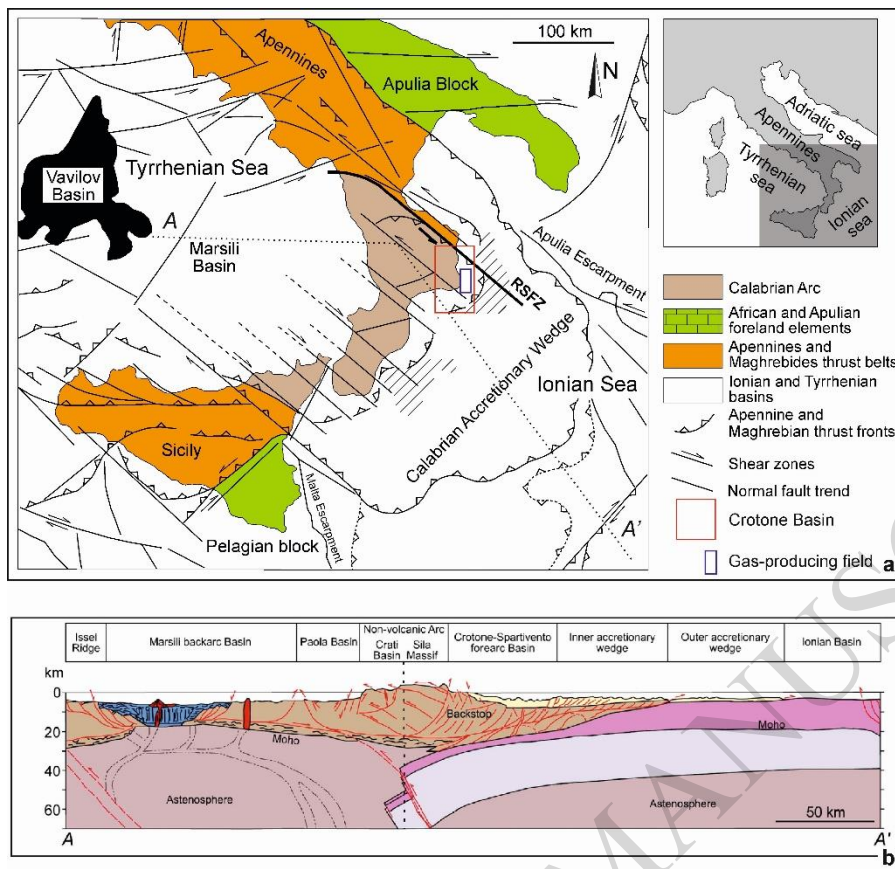


Figure 2

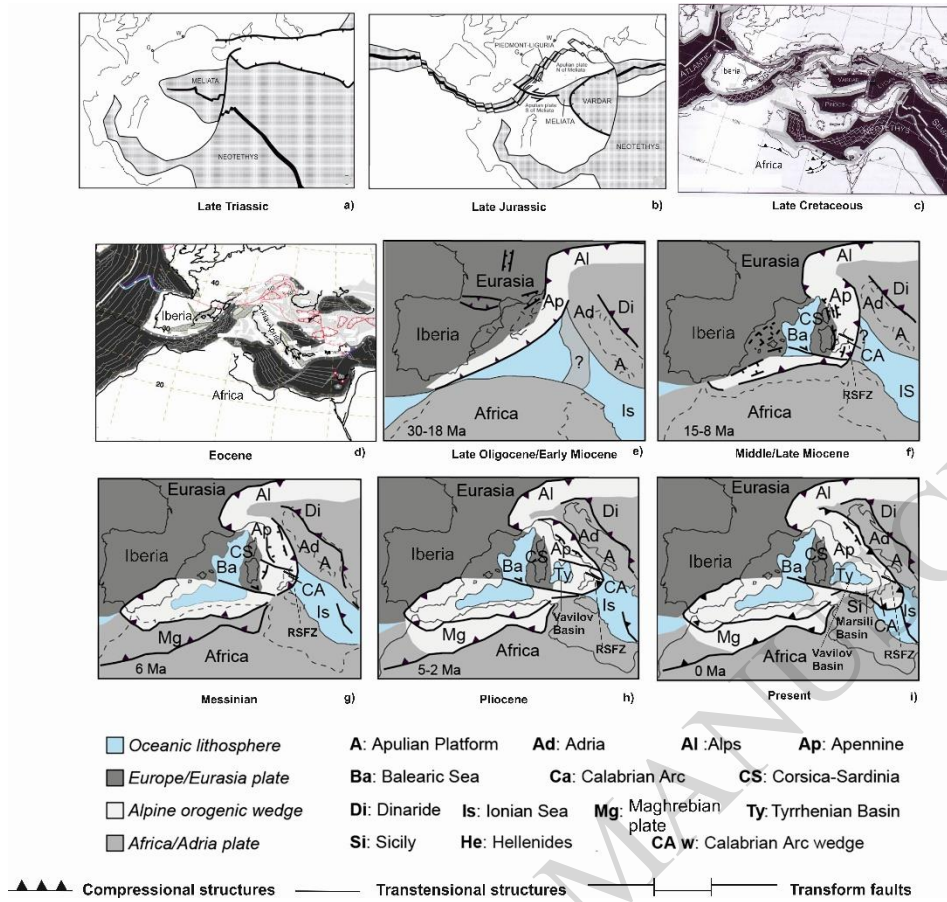


Figure 3

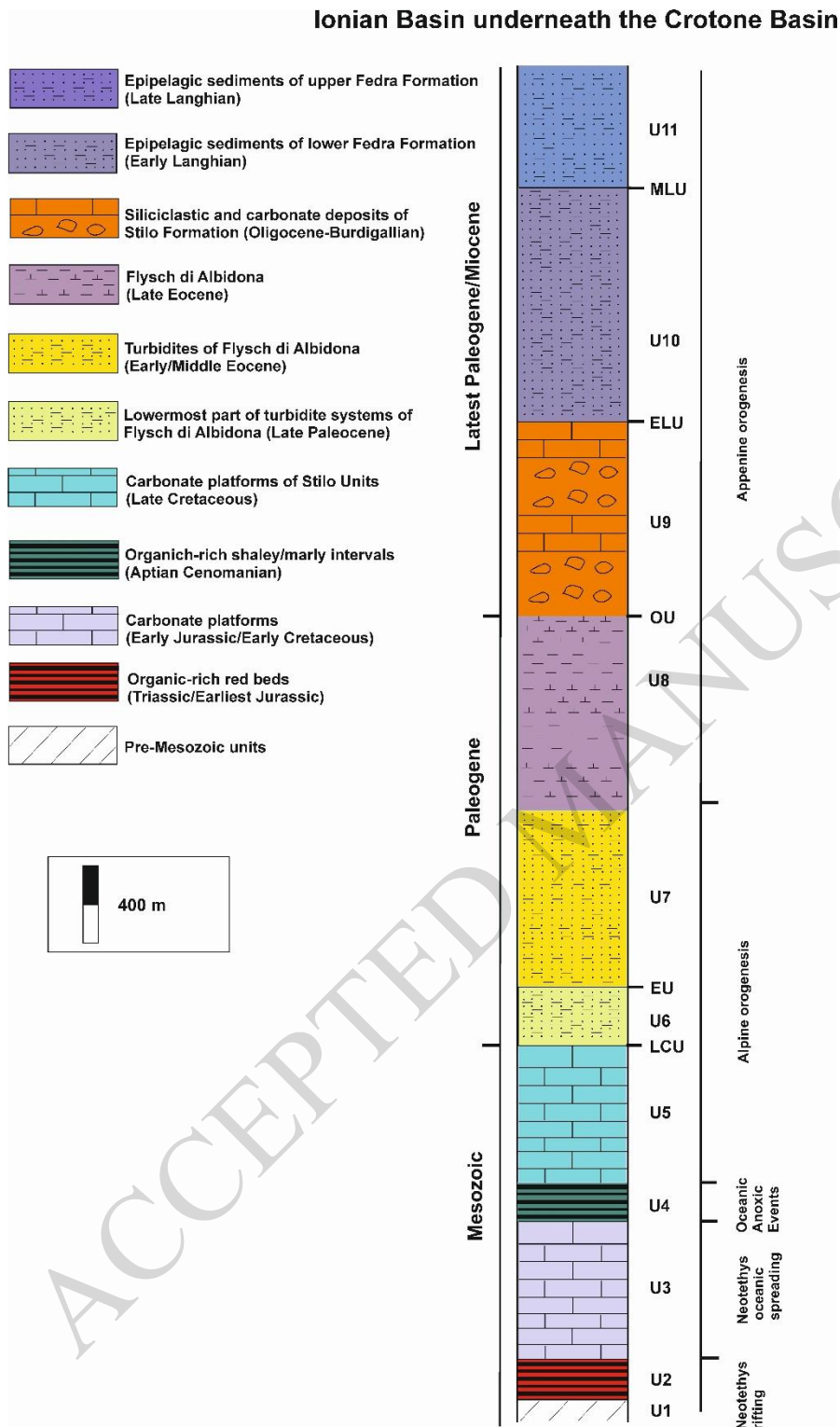


Figure 4

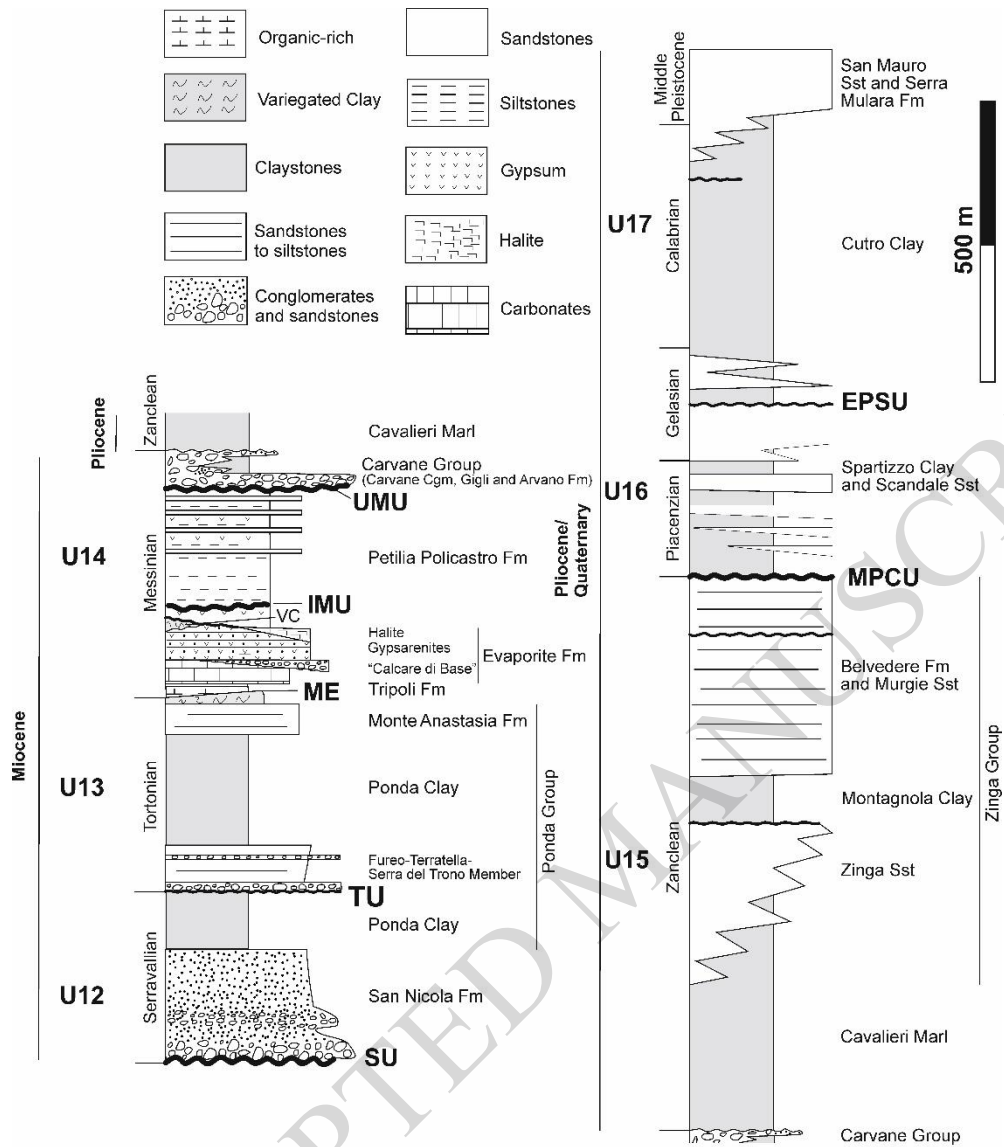


Figure 5

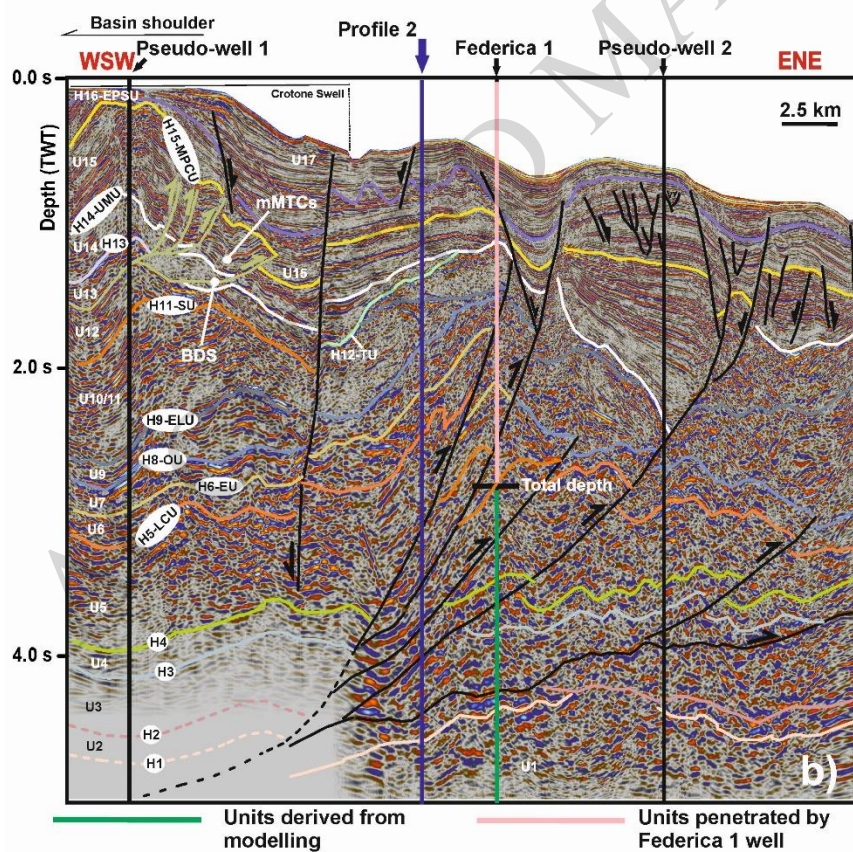
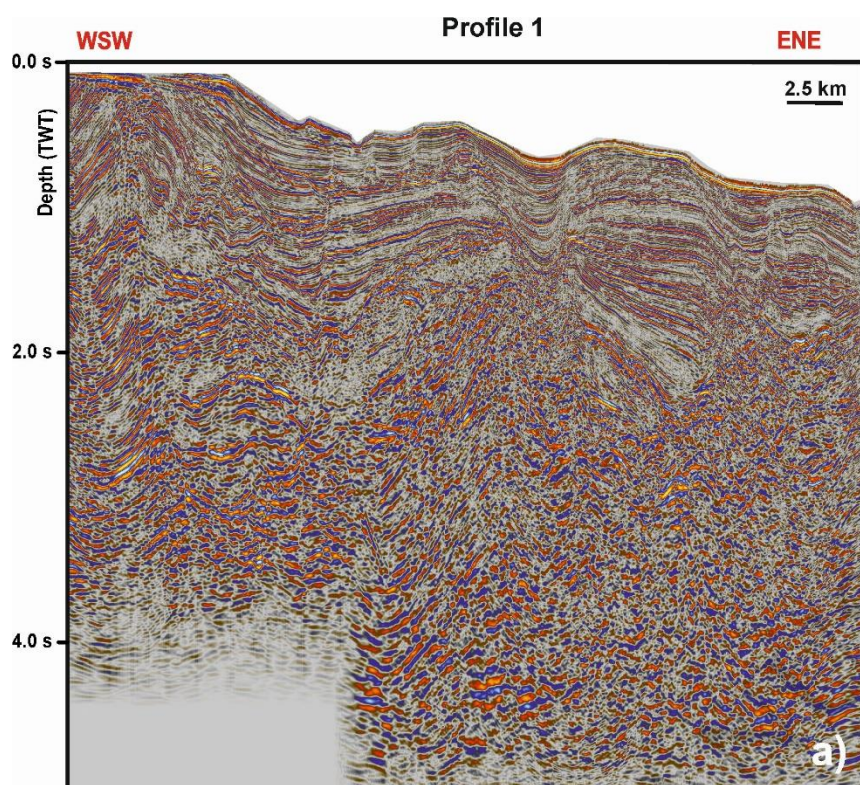


Figure 6

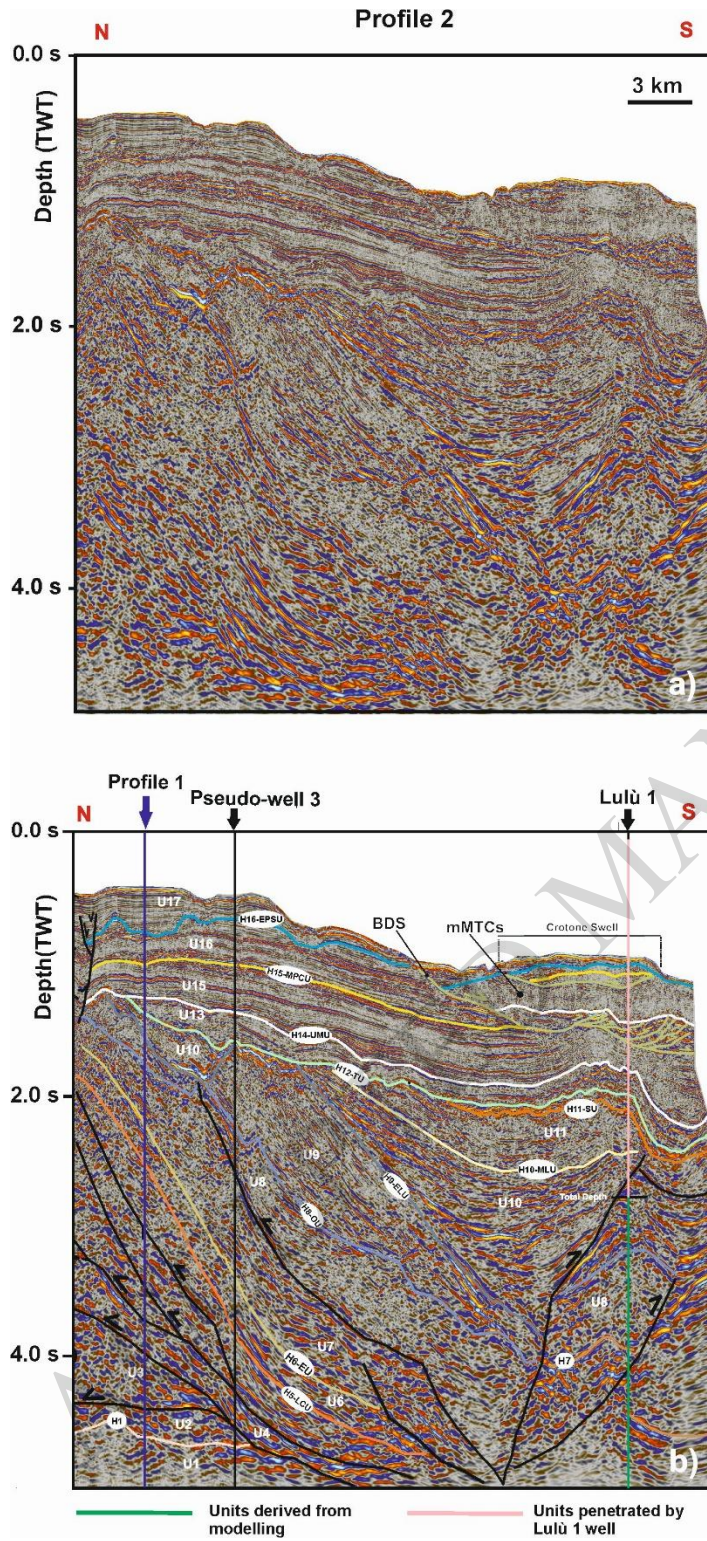


Figure 7

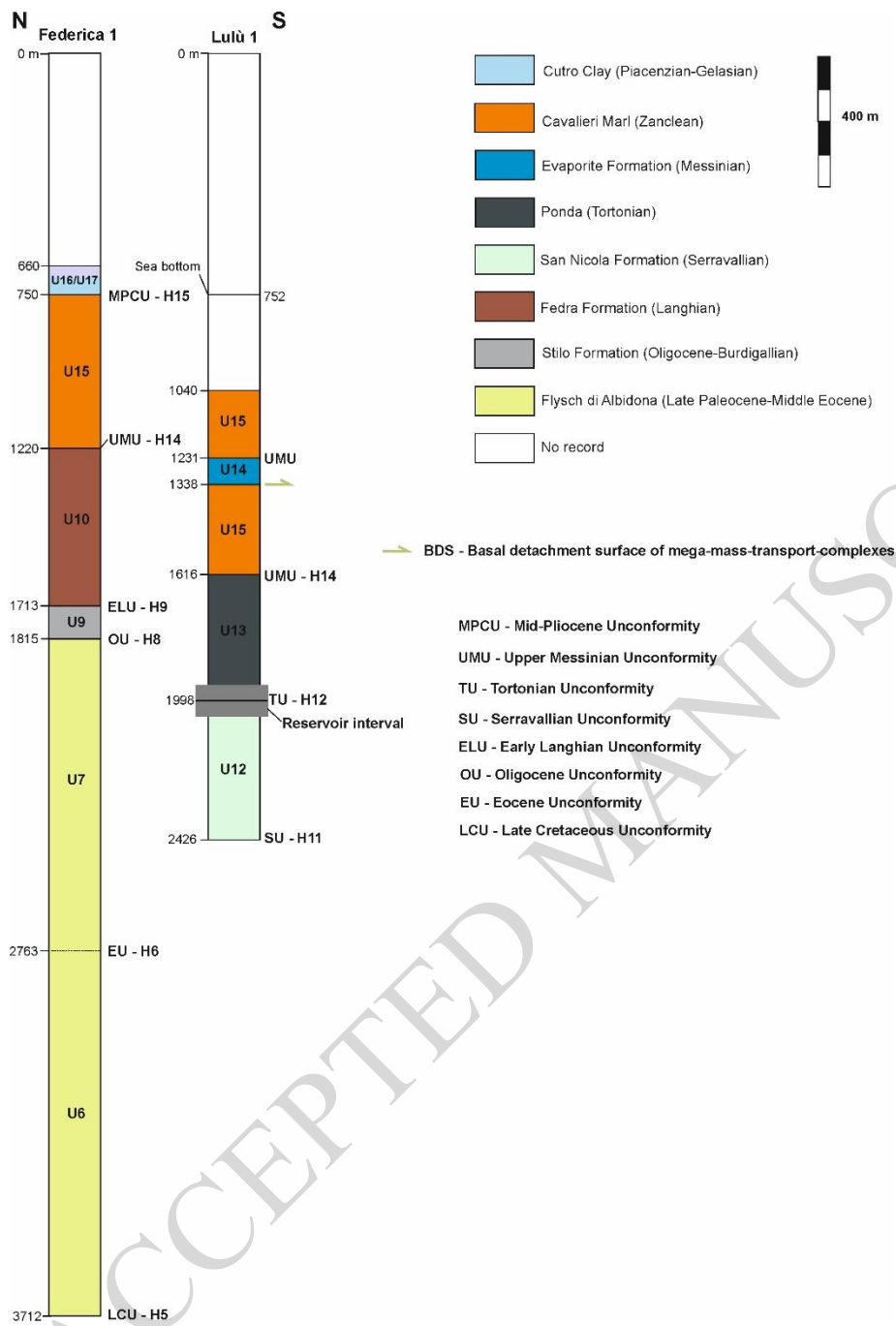
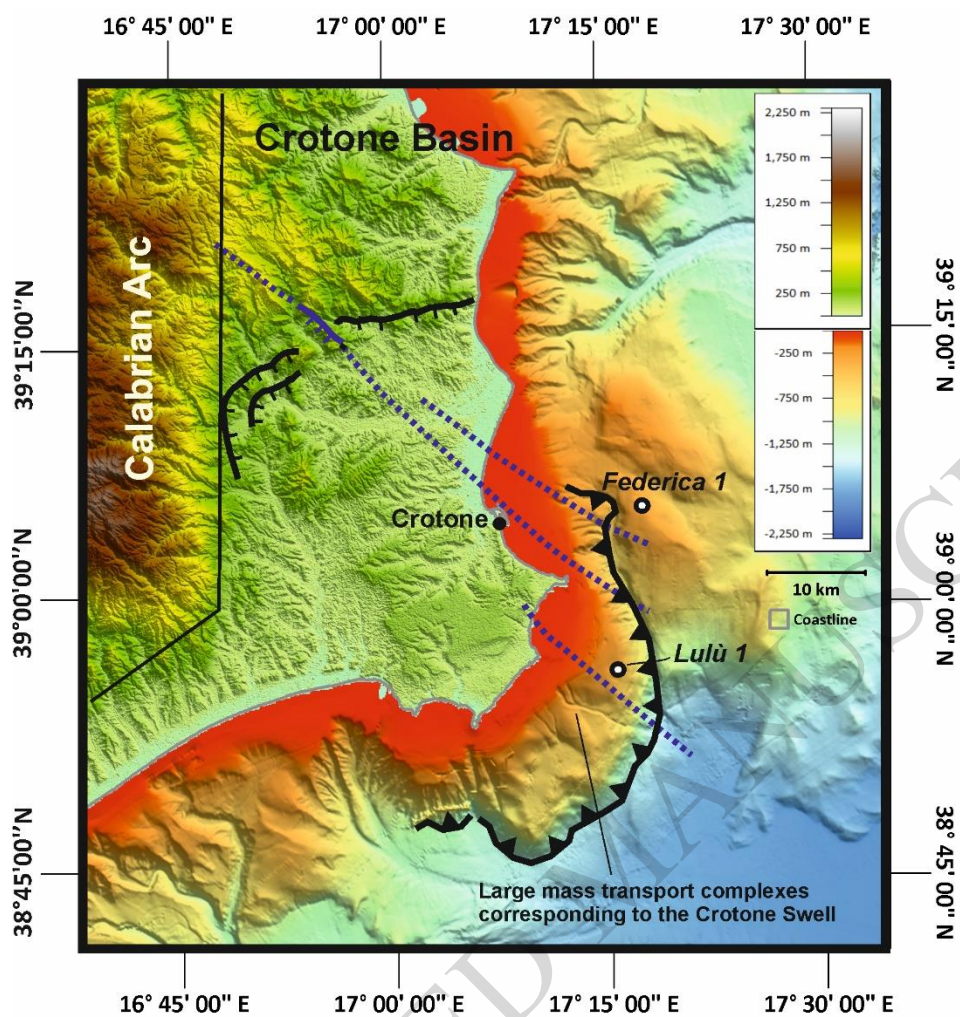


Figure 8








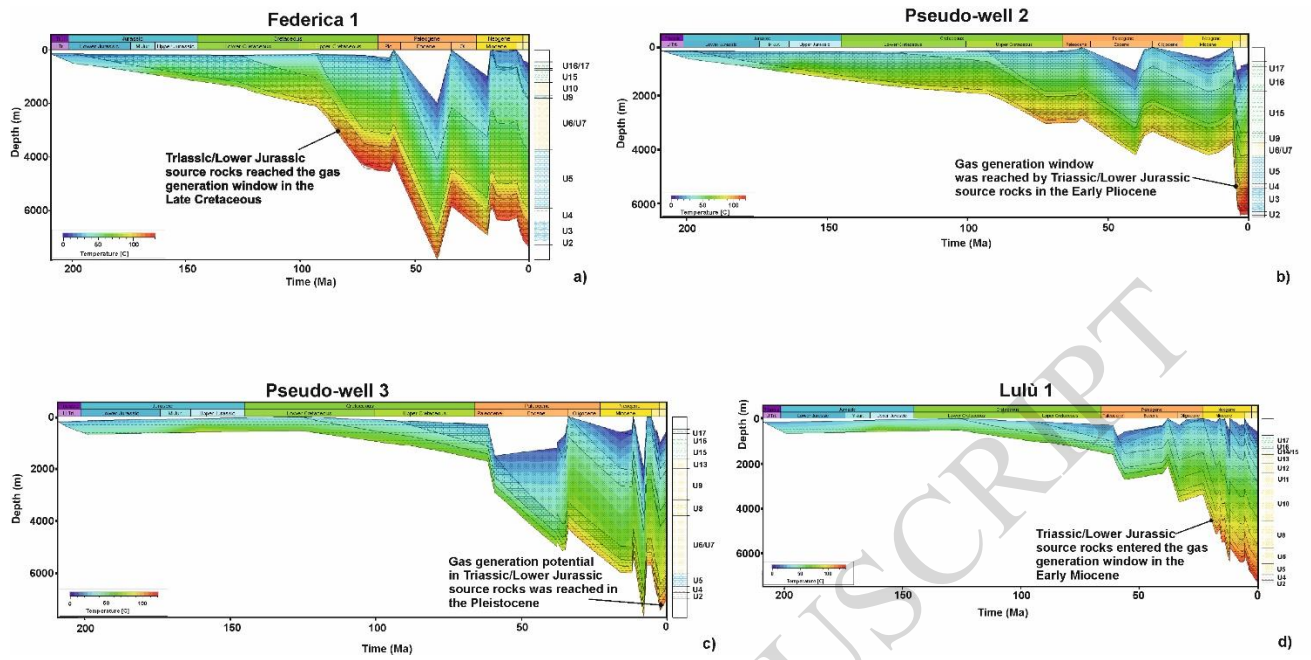
-  Compressional toe of large mass transport complexes
-  Normal faults at large mass transport complex headwall
-  Buried fault segments belonging to the RSFZ
-  Outcropping normal fault segments belonging to the RSFZ
-  Wells

Figure 9



ACCEPTED MANUSCRIPT

Figure 10

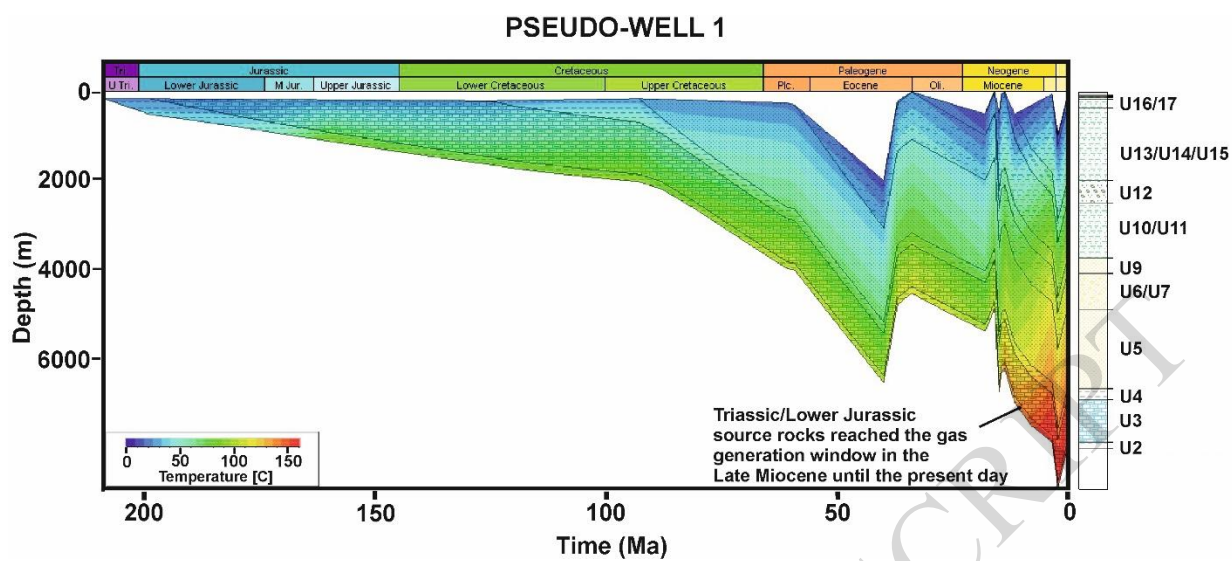


TABLE 1

Unit	Age (Ma)	Lithology	Paleo-water depth (m)	Seawater temperature (°C)	Heat flow (mW/m ²)
U17	0	Siltstones with intercalated sandstones	1000	10	55
U16	2.40	Siltstones with intercalated sandstones	700	10	55
U14/U15	3.60	Siltstones with intercalated sandstones	600	10	56
U13	5.33	Siltstones with intercalated sandstones	800	11	56
U12	11.63	Conglomerates	0	n/a	57
U11	13.82	Siltstones with intercalated sandstones	300	12	57
U10	14.00	Siltstones with intercalated sandstones	300	12	57
U9	15.97	Arkoses	700	13	58
U8	33.90	Marls	750	20	59
U7	41.20	Siltstones with intercalated sandstones	1800	20	60
U6	56.00	Siltstones with intercalated sandstones	1000	21	61
U5	66.00	Carbonates	300	17	63
U4	93.90	Shales with high organic content	100	25	67
U3	125.00	Carbonates	300	22	80
U2	199.00	Shales with high organic content	100	20	62

TABLE 2

Seismic Units	Age of base	TWT Thickness (ms)	Velocity (m/s)	Internal character, geometry and terminations	Lithology	Main geological events
U17	Late Gelasian/Holocene	60-700	2500	Low- to high-amplitude discontinuous sub-parallel reflections. Strongly folded to the WSW, chaotic to the S. Fills depocenters in the distal part. The top is the seafloor. Baselap.	Shelf to slope claystones of Cutro Clay.	Marsiili sub-basin oceanization in the Tyrrhenian at 2.1. Ma.
U16	Piacenzian/Early Gelasian	30-600	2500	Low- to high-amplitude discontinuous internal reflections sub-parallel to wavy, locally chaotic. Highly folded to the WSW. Fills depocenters in the distal area. The top is H16.	Shelf to slope claystones of Cavalieri Marl.	Vavilov sub-basin spreading phase in the Tyrrhenian. H16 corresponds to the EPSU - Early Pleistocene Unconformity. Final collision between the N Calabrian Accretionary Complex and the Apulian plate.
U15	Zanclean	30-1000	2500	Low- to high-amplitude discontinuous internal reflections, chaotic to sub-parallel. Highly folded towards the WSW, fan-like towards the ENE. The top is H15. Baselap and onlap.	Shelf to slope claystones of Cavalieri Marl.	Vavilov sub-basin first spreading in the Tyrrhenian back-arc. H15 correlates MPCU - Mid-Pliocene Unconformity. Collision between the Calabrian Arc and Apulian margin. Emplacement of mMTDs in the basin shoulder.
U14	Messinian	0-350	3000	Low- to high-amplitude discontinuous internal reflections. Highly folded towards the WSW, chaotic towards the ENE, showing compressional structures. The top is H14. Baselap and onlap.	Diatomites, halite, reseedimented evaporites, limestones, siliciclastic conglomerates and mudstones of Evaporite and Petilia Policastro formations	Messinian Salinity Crisis and exposure conditions. The H14 correlates the UMU - Upper Messinian Unconformity. Temporary collision and coupling of the NE part of the Calabrian Arc with the Apulian margin at 5.42 Ma.
U13	Tortonian	0-250	3000	Low- to high-amplitude discontinuous reflectors, wavy to highly folded towards the basin shoulders, locally chaotic. The top is H13 towards the WSW and H14 in the distal area. Baselap and onlap.	Shallow to deep marine siltstones with intercalated sandy and gravelly layers of Ponda Group. It constitutes part of reservoir intervals of the Luna Field.	Subsiding and transgressive conditions. The H13 correlates with the Base of Evaporites.
U12	Serravallian	0-300	2000	Medium- to high-amplitude discontinuous folded reflections. The top is H12. Baselap and onlap.	Fan delta conglomerates and sandstones of San Nicola Formation. Proven reservoir intervals of the Luna Field.	Crotone Basin opening. H12 correlates with the TU - Tortonian Unconformity. Uplift of the basin shoulder.
U11	Late Langhian	0-500	4000	Low to high-amplitude highly discontinuous folded reflections. Locally transparent and chaotic. The top is H11. Baselap and onlap.	Epipelagic sediments of upper Fedra Formation.	H11 correlates with the SU - Serravallian Unconformity. Tectonic uplift of the basin shoulder.
U10	Early Langhian	0-1200	4000	Low- to high-amplitude discontinuous reflections. Folded towards the basin shoulder, concave-up towards the S. The top is H10. Baselap and onlap.	Epipelagic sediments of lower Fedra Formation.	H10 is equivalent to the MLU - Mid-Langhian Unconformity. Appenine orogenesis.
U9	Oligocene/Burdigalian	0-1000	4000	Low- to medium-amplitude discontinuous reflections. Wavy towards the WSW, abruptly inclined towards the S. The top is H9. Baselap.	Siliciclastic and carbonates deposits of Stilo Formation.	H9 correlates with the ELU - Early Langhian Unconformity. Appenine orogenesis.
U8	Late Eocene	0-1000	3000	Low- to medium-amplitude discontinuous reflections. Highly inclined and folded in the distal area. The top is H8 to the N and H9 to the S. Baselap.	Flysch di Albidona.	H8 correlates with the OU - Oligocene Unconformity. Appenine orogenesis.
U7	Early/Middle Eocene	0-900	3000	Low- to medium-amplitude discontinuous reflections, abruptly dipping towards the S. Locally wavy. The top is H8. Baselap.	Turbidites of Flysch di Albidona.	Alpine orogenesis.
U6	Late Paleocene	0-300	3000	Medium- to high-amplitude discontinuous reflections. Wavy towards the basin shoulder, abruptly inclined towards the S. The top is H6. Baselap.	Lowermost part of turbidite system of Flysch di Albidona.	The H6 correlates with the EU - Eocene Unconformity. Alpine orogenesis.
U5	Late Cretaceous	0-2000	2500	Low- to high-amplitude seismic discontinuous reflections. Wavy towards the basin, steeply dipping towards the S. The top is H5. Baselap.	Carbonate platforms of Stilo Units.	H5 correlates with the LCU - Late Cretaceous Unconformity. Alpine orogenesis.
U4	Aptian/Cenomanian	200	2200	Low- to high-amplitude undulated discontinuous reflections. The top is H4. Baselap.	Organich-rich shaly/marly intervals gas source.	Oceanic Anoxic Events (OAEs).
U3	Early Jurassic/Early Cretaceous	0-700	2500	Low- to medium amplitude undulated reflections. The top is H3. Baselap.	Carbonate platforms.	Neothetys oceanic spreading.
U2	Triassic/Earliest Jurassic	0-200	2200	Low- to medium poorly stratified reflections. The top is H2. Onlap.	Organich-rich redbeds.	Neothetys rifting.
U1	Pre-Mesozoic	0-1000		Transparent discontinuous internal reflections.		